AGU PUBLICATIONS

Reviews of Geophysics

REVIEW ARTICLE
10.1002/2015RG000505

Key Points:
- This paper reviewed the studies of upwelling in the China seas conducted since 2000
- Upwelling dynamics with applications to the China seas have been summarized
- Considerations on further upwelling studies have been proposed

Correspondence to:
J. Hu,
hujy@xmu.edu.cn

Citation:
Hu, J., and X. H. Wang (2016), Progress on upwelling studies in the China seas, *Rev. Geophys.*, *54*, 653–673, doi:10.1002/2015RG000505.

Received 30 SEP 2015
Accepted 17 JUL 2016
Accepted article online 21 JUL 2016
Published online 17 SEP 2016

Progress on upwelling studies in the China seas

Jianyu Hu[1] and Xiao Hua Wang[2]

[1]State Key Laboratory of Marine Environmental Science, College of Ocean and Earth Sciences, Xiamen University, Xiamen, China, [2]Sino-Australian Research Centre for Coastal Management, University of New South Wales, Canberra, ACT, Australia

Abstract East Asian marginal seas surrounding China exhibit rich ocean upwelling, mostly in response to the southwesterly summer monsoon. Upwelling in the China seas, namely, the South China Sea, the Taiwan Strait, the East China Sea, the Yellow Sea, and the Bohai Sea, has become increasingly important because the potential changes in the upwelling may have dramatic ecosystem, socioeconomic, and climate impacts. This paper reviews the progress of upwelling studies in the China seas since the year 2000, by presenting the principal characteristics and new understanding of 12 major upwelling regions in the China seas. Upwelling exhibits long-term variability at intraseasonal to multidecadal scales as well as short-term variability frequently caused by tropical cyclones. It is also associated with the El Niño–Southern Oscillation, local environmental variation, and biogeochemical factors. The coastal upwelling around Hainan Island and the upwelling or cold dome northeast of Taiwan Island are specifically highlighted because they have attracted great interest for decades. This paper summarizes upwelling mechanisms in terms of wind, topography, tide, stratification, and background flow, with applications mostly to the China seas. Finally, we propose some topics for future upwelling research, i.e., potential intensification of coastal upwelling under global climate change, downwelling, intrusion of upwelling into coastal embayments, and the influence of upwelling on fishery and biogeochemical processes.

1. Introduction

Upwelling in the ocean is defined as an upward movement of seawater, with a speed ranging from about 10^{-6} to 10^{-4} m/s. As upwelled water carries a large amount of nutrients (such as phosphate and nitrate) from the lower layer to the upper layer or even to the surface layer of the ocean, upwelling regions generally are important fishing areas. Upwelling, with relatively high chlorophyll (Chl *a*) concentration and relatively low sea surface temperature (SST), as is commonly observed in the China seas [*Wei et al.*, 2008; *Xiong et al.*, 2012], is also of major importance to primary and secondary productivity and strongly influences atmosphere-ocean CO_2 exchange and carbon recycling [*McGregor et al.*, 2007]. Figure 1 illustrates monthly mean SST in August 2013 and presents several upwelling-related low SST regions in the China seas.

The China seas (Figure 2), namely, the South China Sea (SCS), the Taiwan Strait (TWS), the East China Sea (ECS; or the Donghai Sea), the Yellow Sea (or the Huanghai Sea), and the Bohai Sea, are located in the northwestern Pacific Ocean. Upwelling in the China seas is usually induced by winds and is largely affected by local circulation, topography, and tides.

Being in the subtropical monsoon regime, the China seas are characterized by distinctly seasonal variation of winds. In winter, these seas are predominantly controlled by northeasterly and northerly winds. In summer, the SCS is dominated by southwesterly and southerly winds, while the ECS, the Yellow Sea, and the Bohai Sea are governed by southerly and southeasterly winds (Figure 1) [e.g., *Zheng*, 2011; *X. Y. Chen et al.*, 2014].

The circulation in the China seas includes the Kuroshio Warm Current system, the China Coastal Current system, and some local currents or gyres, as shown in Figure 3 [e.g., *Zheng et al.*, 2006]. The circulation in the ECS, the Yellow Sea, and the Bohai Sea usually flows in an anticyclonic pattern [e.g., *Isobe*, 2008]. Specifically, the Kuroshio flows northeastward in the eastern ECS and the subsurface water of the Kuroshio northeast of Taiwan may intrude to the coast of Zhejiang and contribute to the formation of upwelling there in summer (Figure 4) [*Yang et al.*, 2011, 2013]. The coastal current does not mainly depend on the wind field in the Yellow Sea but differs from season to season in the ECS.

There are three currents in the TWS: the China Coastal Current along the western TWS, the extension of the SCS Warm Current in the western and central TWS, and the Kuroshio's branch or loop current intruding through the eastern TWS [*Hu et al.*, 2010]. The latter two currents play significant roles in the upwelling in

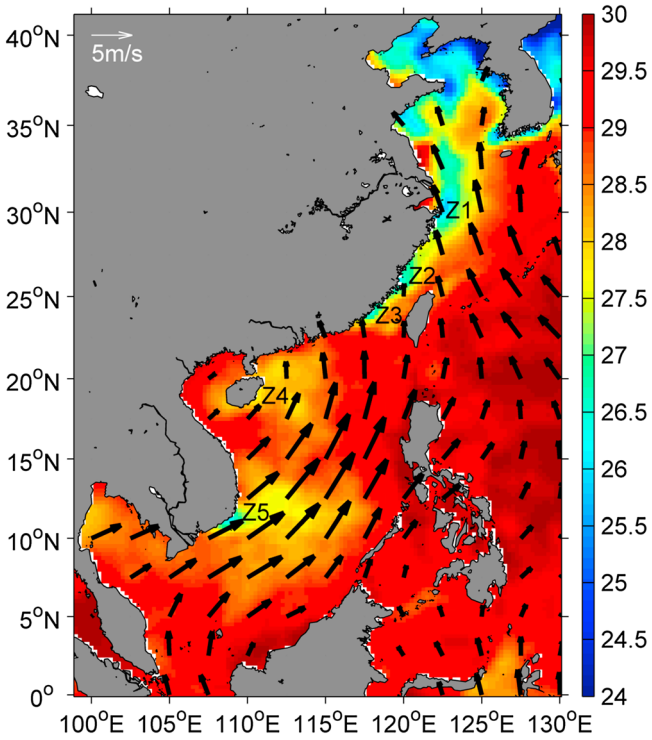

Figure 1. Monthly mean sea surface temperature (SST, in °C) and wind (vector, in m/s) in August 2013. The illustration is made from the daily Optimum Interpolation Sea Surface Temperature data and monthly National Centers for Environmental Prediction reanalysis wind data produced by the National Oceanic and Atmospheric Administration (NOAA). Z1, Z2, Z3, Z4, and Z5 in the figure represent five relatively low SST zones associated with the coastal upwelling in the China seas.

the TWS [*Hu et al.*, 2003b]. However, these currents exhibit differences between winter and summer seasons and between upper and lower layers.

The upper layer circulation of the SCS is cyclonic in winter but anticyclonic in summer [*Hu et al.*, 2000; *Gan et al.*, 2006]. In winter, two cyclonic eddies exist west of Luzon Island (Luzon cold eddy) and in the southwestern SCS, respectively. In summer, a coastal jet forms between an anticyclonic eddy in the southwestern SCS and another cyclonic eddy (Vietnam cold eddy) off the central coast of Vietnam [e.g., *Gan and Qu*, 2008]. In addition, the northern SCS circulation pattern is modified by including the SCS Warm Current, the seasonal Kuroshio intrusion, and some mesoscale eddies, which accordingly modulate the upwelling in the northern SCS.

Previous studies on the upwelling in the SCS and the TWS have been summarized mainly in two review papers by *Wu and Li* [2003] and *Hu et al.* [2003b], respectively. These authors collected several decades of research results on upwelling, mostly before 2000. However, our understanding of the characteristics and mechanisms of upwelling and its variability in the China seas has significantly progressed since 2000.

This review paper documents the progress of upwelling studies in the China seas during 2000–2015 (sections 2.1 and 2.2) and presents a summary of the upwelling studies in the China seas (section 2.3). In section 3, the dynamics of the upwelling studies are specifically summarized and discussed. Finally, in section 4, we propose some considerations about further studies on upwelling that are of global significance and of great interest to the broad community.

2. Progress of Upwelling Studies in the China Seas

2.1. Characteristics of Major Upwelling Regions in the China Seas

2.1.1. Upwelling in the South China Sea

Wu and Li [2003] summarized the upwelling research in the SCS during the 40 years of 1964–2003 and emphasized the temporal and spatial distributions of upwelling in the northern SCS. Their review concluded that the upwelling covers almost the entire northern continental shelf of the SCS in summer. Since 2000, several cruises acquiring hydrographical or comprehensive observations have been conducted in the northern SCS. These cruise data further indicated that the coastal upwelling appears earlier and is stronger along the eastern Guangdong coast than along the southern Fujian coast [e.g., *Xu et al.*, 2013, 2014]. Moreover, satellite remote sensing SST and Chl *a* data from different sources demonstrated that the upwelled water in the surface layer of the Guangdong coast can appear in a jet-like wedge shape [*Gu et al.*, 2015].

Through the recent decade, much attention was paid to the coastal upwelling along the coast of Vietnam (Vietnam coastal upwelling) [e.g., *Barthel et al.*, 2009; *Dippner and Loick-Wilde*, 2011] and the cold eddy off central Vietnam (Vietnam cold eddy) [e.g., *He et al.*, 2002; *Guo et al.*, 2006]. Climatological temperature and

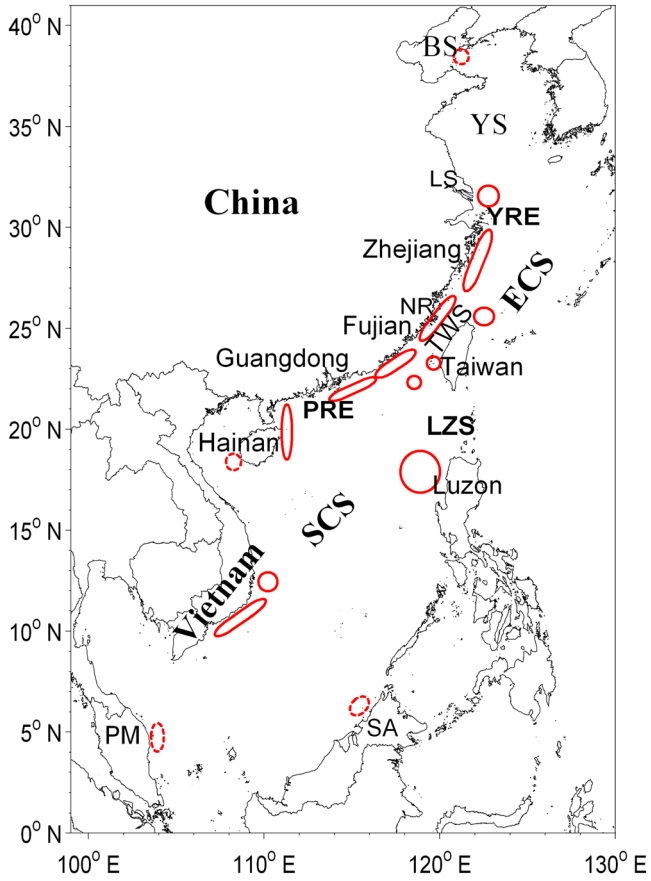

Figure 2. Map of the China seas, including the South China Sea (SCS), the Taiwan Strait (TWS), the East China Sea (ECS), the Yellow Sea (YS), and the Bohai Sea (BS). In the figure, the Yangtze River Estuary and the Pearl River Estuary are indicated by YRE and PRE, respectively. PM stands for the Peninsular Malaysia; LZS for Luzon Strait; and LS, NR, and SA for Lüsi, Nanri, and Sabah, respectively. The red ellipses or circles schematically mark locations of the major upwelling regions in the China seas. The ellipses or circles in dashed lines are upwelling regions that are sometimes mentioned.

salinity data [*Boyer et al.*, 2005] have indicated that the summertime low-temperature center in the western SCS varies spatially at different depths; i.e., the surface low-temperature (and high-salinity) center is located in the shallow region along the eastern and southeastern Vietnam coast, but the low-temperature (and high-salinity) center in the subsurface layer appears offshore below 200 m [*Zhuang et al.*, 2006]. The former is regarded as the Vietnam coastal upwelling, whereas the latter is regarded as the Vietnam cold eddy. The centroid of upwelling-generated cold water moves southward from 15°N in May to 11°N in August with a changing of the upwelling scale, and the cold water finally evolves into a cold jet stretching offshore in mid-August [e.g., *Kuo et al.*, 2000; *Xie et al.*, 2003]. The coastal upwelling area can also be seen along the coast of southern Vietnam in the maps of climatological monthly mean SST from the World Ocean Database 1998 [*Petrichenko*, 2010]. The cold eddy off Vietnam is characterized as one dynamically active area (12–13°N, 110–112°E) with lowest sea surface height in August [e.g., *Ho et al.*, 2000a; *Wang et al.*, 2003]. Hydrographical data have revealed the features and the three-dimensional structure of this cold eddy [e.g., *Fang et al.*, 2002; *Hu et al.*, 2011b].

The upwelling off the northwestern coast of Luzon Island is usually observed as a cold eddy, named the Luzon cold eddy. This cyclonic eddy has been identified off northwestern Luzon Island by altimeter data [e.g., *Ho et al.*, 2000b; *Hwang and Chen*, 2000], by historical temperature and salinity data [e.g., *Qu*, 2000; *Udarbe-Walker and Villanoy*, 2001], and by a total of 105 years of observational data in the SCS [*Liu et al.*, 2006]. The eddy exists for 7 months from October to the following May, developing in October–November, intensifying in December–January, and decaying in February–May. It covers an area from 16° to 19°N and from 117° to 120°E (Figure 5) and reaches maximum size during its intensification period. Additional evidence has shown that this cyclonic eddy sometimes has two or three cold cores off western Luzon Island [*Yuan et al.*, 2004; *Sun and Liu*, 2011].

2.1.2. Upwelling in the Taiwan Strait

Xiao et al. [2002] and *Hu et al.* [2003b] systematically reviewed the advances attained through upwelling studies in the TWS, mostly before 2000 [e.g., *Chen et al.*, 1982], and proposed several directions for future efforts. Many hydrological measurements [e.g., *Wan et al.*, 2013; *Zhu et al.*, 2013] and satellite observations acquired during the last 15 years [e.g., *Tang et al.*, 2002; *Shang et al.*, 2004] and numerical models developed during this period [e.g., *Pan and Sha*, 2004] have further confirmed that two regions of coastal upwelling in the southwestern and northwestern TWS usually appear during the summertime southwesterly monsoon period and that another two regions of upwelling around the Taiwan Bank and the Penghu Islands exist all year round. For example, observations showed that evident coastal upwelling appeared in the southwestern

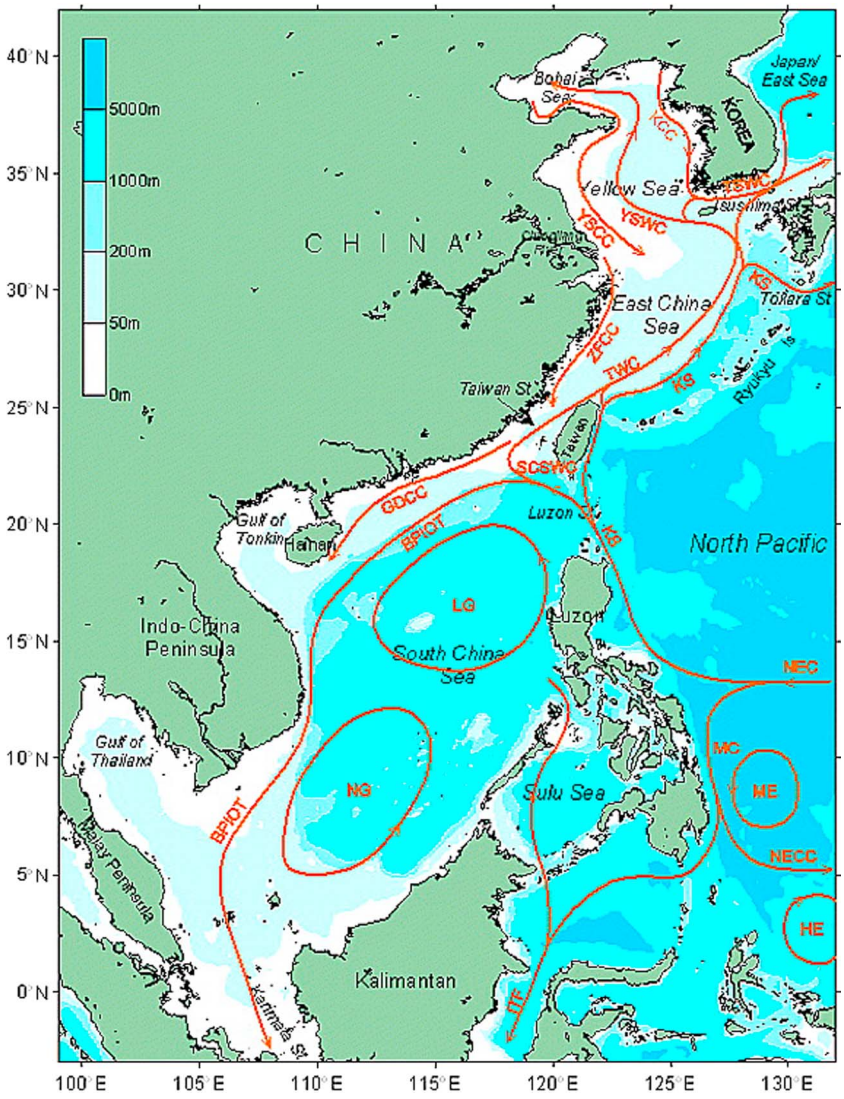

Figure 3. Topography and schematic representation of the major winter currents in the China seas and their adjacent waters (cited from *Zheng et al.* [2006, Figure 1]). This current system diagram is a composite based mainly on some previous research. The abbreviations used only in this figure are the following: BPIOT, Branch of the Pacific-to-Indian Ocean Throughflow; GDCC, Guangdong Coastal Current; HE, Halmahera Eddy; ITF, Indonesian Throughflow; KCC, Korea Coastal Current; KS, Kuroshio; LG, Luzon Gyre; MC, Mindanao Current; ME, Mindanao Eddy; NEC, North Equatorial Current; NECC, North Equatorial Countercurrent; NG, Nansha Gyre; SCSWC, South China Sea Warm Current; TSWC, Tsushima Warm Current; TWC, Taiwan Warm Current; YSCC, Yellow Sea Coastal Current; YSWC, Yellow Sea Warm Current; and ZFCC, Zhejiang-Fujian Coastal Current.

TWS in July 2005 and July 2007 [*Hu et al.*, 2011a] and that the upwelling-related surface cold water existed near Dongshan in early July 2004, diminished to half its original size with decreased Chl *a* concentration 15 days later, and disappeared by the end of July [*Zhang et al.*, 2011].

2.1.3. Upwelling in the East China Sea

Coastal upwelling phenomena in the ECS have been observed along the Zhejiang coast and in the Yangtze River (or Changjiang River) Estuary. In the Yangtze River Estuary, there exists upwelling with a scale of about 1° in longitude and 1° in latitude centered around (31°30′N, 122°40′E) [*Zhao et al.*, 2001]. Signals of low-temperature and high-salinity upwelling water in the Yangtze River Estuary appeared at three sections of the temperature and salinity distributions (Figure 6) obtained from a cruise in August 2000 [*Zhu*, 2003; *Zhu et al.*, 2003; *Lü et al.*, 2006]. Evidently, the high-salinity water can upwell toward 5–10 m layer from the lower layer and affect the salinity distribution in the Yangtze River Estuary. Along the Zhejiang coast, upwelling

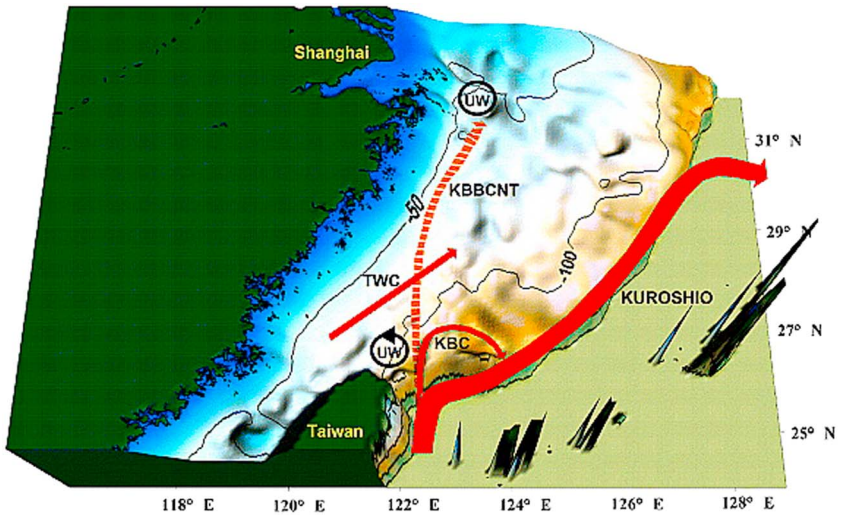

Figure 4. Summer ocean circulation pattern in the ECS. The solid thin lines represent the 50, 100, 200, and 500 m isobaths. The dashed red line represents the possible ocean current of the Kuroshio Bottom Branch Current to the northeast of Taiwan (KBBCNT). The red lines show the Kuroshio, the Kuroshio Branch Current (KBC), and the Taiwan Warm Current (TWC), and UW denotes upwelling. Cited from Figure 19 of *Yang et al.* [2011].

appears in June, develops to its strongest condition in July and August, and then weakens and eventually vanishes in late September [*Lou et al.*, 2011]. The low SST in the upwelling region is about 24–27°C in summer, and the temperature difference from its surrounding nonupwelling waters ranges from 2 to 4°C [*Hu and Zhao*, 2008; *Lou et al.*, 2011]. In addition, the upwelling in the ECS has also been simulated by many numerical models [e.g., *Qiao et al.*, 2006; *Jing et al.*, 2007].

Another upwelling region is located in the shelf break area of the ECS, where a distinct cold eddy was observed from the hydrological and chemical data obtained during two cruises [*Qiao et al.*, 2008], which revealed a ring-like structure; i.e., the maximum upwelling speed did not appear near the center of the cold eddy but at a small distance from the center.

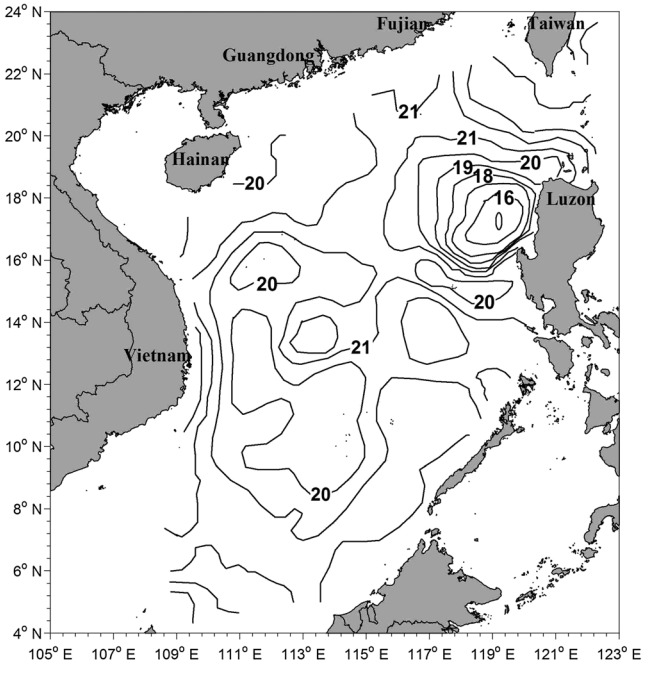

Figure 5. Temperature distribution (°C) at 100 m in the SCS in January. Redrawn from Figure 3 of *Liu et al.* [2006].

2.2. New Understandings of the Upwelling in the China Seas Since 2000

2.2.1. Upwelling Variability: Intraseasonal to Multidecadal Scale

Long-term analysis of satellite SST, Chl *a*, and wind data sets showed that the upwelling has annual and interannual variations along the Fujian and Zhejiang coasts and in the Yangtze River Estuary [e.g., *Tang et al.*, 2004a; *Hu and Zhao*, 2007]. For the summer coastal upwelling in the TWS, a long time series of SST data indicated that the coastal upwelling near Pingtan or Dongshan had a signature of cold and saline upwelling water at the surface in some years during 1985–2005 but no signature of upwelling water at the surface in the other years [*Hong et al.*, 2009]. This variability is closely correlated with the variation in the

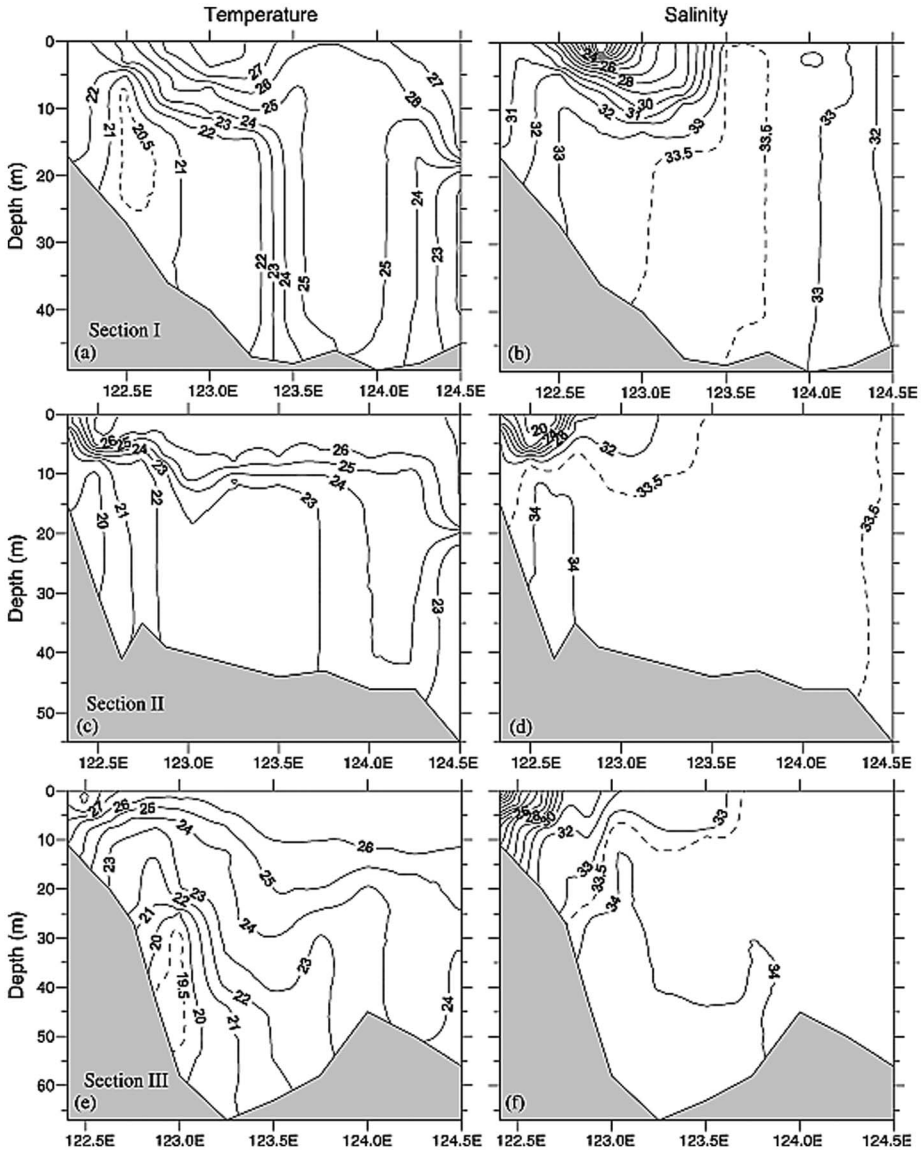

Figure 6. Vertical distributions of (a, c, and e) temperature (°C) and (b, d, and f) salinity along Section 32.0°N (Figures 6a and 6b), Section 31.5°N (Figures 6c and 6d), and Section 31.0°N (Figures 6e and 6f) in the Yangtze River Estuary. The interpolated contours are shown as dashed lines. Cited from Figure 3 of *Lü et al.* [2006].

alongshore component of wind stress. Such variability of coastal upwelling can also be demonstrated by a variable hydrographical structure in the sea area near Dongshan with different scale, location, and intensity of low-temperature and high-salinity water [*Hu et al.*, 2011a]. In addition to interannual variability, two regions of coastal upwelling in the western TWS have clear intermonthly variability in summer [*Hu et al.*, 2001], and the coastal upwelling and cold eddy off Vietnam are punctuated by the intraseasonal oscillation [e.g., *Xie et al.*, 2007].

Long-term variability of upwelling is usually associated with the El Niño–Southern Oscillation (ENSO). As the sea surface wind was much weaker in the TWS during the 1997 El Niño year than during the 1998 La Niña year [*Kuo and Ho*, 2004], the coastal upwelling in the TWS was correspondingly weak and strong in summers of 1997 and 1998, respectively [e.g., *Hong et al.*, 2011b]. The coastal upwelling in the northern SCS was also significantly strengthened during the summer of 1998 (a La Niña year) when the alongshore wind stress was dramatically enhanced over the region [*Jing et al.*, 2011]. However, a recent research also proposed that the summer SST in the SCS is correlated with ENSO in the preceding winter [*Yang et al.*, 2015]. The coastal

upwelling in the western SCS is strong with the center moving southward in an El Niño year (such as 1997 and 2003) but weak in a La Niña year (such as 1998) [e.g., *Kuo et al*., 2004; *Hein et al*., 2013]. The Luzon cold eddy has significant interannual variation and is highly correlated to the ENSO events, as demonstrated by an extra-strong basin-wide warming in the summer of 1998 that persisted until autumn and winter and prevented the formation of winter upwelling off Luzon in that year [*Wu and Chang*, 2005].

The prominent multidecadal variability of upwelling in the northern SCS has been driven by Asian summer monsoon dynamics, with an abrupt transition from a warmer to a colder condition in 1930 and a return to a warmer condition after 1960 [*Liu et al*., 2013]. In addition, an oscillation of coastal upwelling with significant fluctuations on interannual and decadal scales has been revealed off eastern Hainan Island [e.g., *Liu et al*., 2009; *Su et al*., 2013].

2.2.2. Upwelling Variability: Upwelling or Cold Eddy Induced by Tropical Cyclones

Short-term variability of upwelling can be caused by the tropical cyclones (including typhoons) frequently passing over the SCS and the ECS each year. Responses of the upper ocean to tropical cyclone have been studied extensively for the past 15 years [*Chen et al*., 2013]. One pioneer work in the SCS demonstrated the oceanic response to tropical cyclone Ernie in 1996, indicating an intense upwelling at the subsurface layer and an evident surface cooling to the right of the storm track [*Chu et al*., 2000]. Since 2000, much additional related research has been conducted using in situ data, remote sensing data, and numerical models. For example, several numerical results showed that (1) the typhoon-induced upwelling is responsible for 84% of the cooling in the lower surface layer (40–70 m) [*Wang and Qiao*, 2008] and (2) the SST can drop by 2–6°C in a rightward-biased response to typhoon [*Cui et al*., 2009; *Jiang et al*., 2009].

A cold eddy is generally induced when a typhoon moves in a loop form over the SCS [*Hu and Kawamura*, 2004]. An increasing number of cases have further revealed the oceanic responses to various tropical cyclones in the SCS [e.g., *Shang et al*., 2008; *Su et al*., 2011; *Yang et al*., 2012]. For instance, one showed that a classic cooling anomaly usually occurs to the right of the storm track during the typhoon forced period and that cold anomaly water also exists toward the left of the storm track in the typhoon relaxation period around the Luzon Strait [*Kuo et al*., 2011]. One other case indicated that the coastal upwelling along the eastern Guangdong coast is sensitive to subtle changes in typhoon intensity and path [*Pan et al*., 2012b]. Yet another showed that ocean mixed layer deepening, which is regarded as an important parameter characterizing upwelling and turbulent mixing driven by strong typhoon wind, can be seen after typhoon passage over the SCS [*Pan and Sun*, 2013]. In addition, the thermocline depth is a major factor for the tropical cyclone-induced SST cooling. In particular, the cooling in the SCS is more than 1.5 times that in the tropical northwestern Pacific Ocean because of a shallower mixed layer and stronger subsurface thermal stratification in the SCS [*Mei et al*., 2015].

In the ECS, typhoon-induced oceanic cooling or upwelling is complicated by the presence of the continental shelf of the ECS and the Kuroshio [*Chen et al*., 2003; *Tsai et al*., 2008]. The upwelling caused by a typhoon east of Taiwan can induce an east-west sea level difference that enhances the Kuroshio in the area [*Morimoto et al*., 2009].

Typhoon Kai-Tak, which traversed the northeastern SCS in July 2000, was a typical typhoon that has attracted much interest. Cold patches, with anomalous cooling of up to 6°C below the surrounding warm tropical ocean, formed in the SCS in the trail of the typhoon [*Lin et al*., 2003b]. Additional evidence showed that Typhoon Kai-Tak triggered an average thirtyfold increase in surface Chl *a* concentration, which contributed to 2–4% of the SCS's annual new production [*Lin et al*., 2003a]. A basin-scale ocean model was used to simulate the oceanic response to Typhoon Kai-Tak, and it obtained a drop in SST of more than 9°C, which was attributed to the influence of the slow-moving typhoon, initial stratification, and bathymetry-induced upwelling [*Tseng et al*., 2010]. The upwelling and entrainment induced by Typhoon Kai-Tak accounted for 62% and 31% of the SST drop, respectively, so the upwelling contribution was twice the vertical entrainment contribution [*Chiang et al*., 2011]. Clearly, Typhoon Kai-Tak produced a record SST drop of about 10.8°C (Figure 7) and a high Chl *a* concentration because it passed over a cold eddy with anomalously shallow thermocline at the "right time."

2.2.3. Upwelling East and Northeast of Hainan Island

The upwelling off the eastern coast of Hainan Island is strong in summer, which has attracted a lot of attention in recent years [*Xie et al*., 2012]. It has been revealed that the coastal upwelling begins in April, becomes

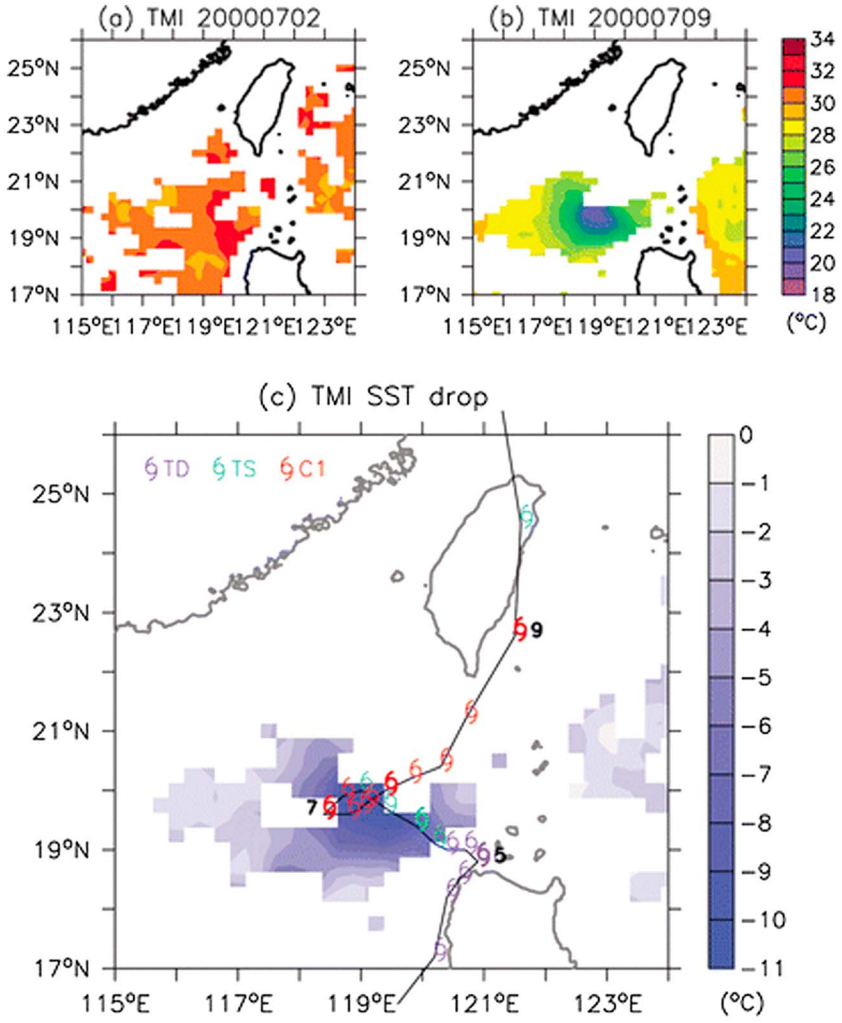

Figure 7. The Tropical Rainfall Measuring Mission Microwave Imager (TMI) daily SST images (ascending) on (a) 2 July and (b) 9 July and (c) SST drop between 2 July and 9 July with the Typhoon Kai-Tak track on selected dates indicated and with intensity marked 6-hourly from the Joint Typhoon Warning Center best track data (available online at http://www.usno.navy.mil/JTWC). Cited from Figure 2 of *Chiang et al.* [2011].

strongest in summer (peaking from mid-July to mid-August), and remains evident until September, that the upwelling-favorable wind is the main driving force, and that the alongshore topographic variation plays an important role in generating upwelling centers distributed along the eastern Hainan coast [e.g., *Su and Pohlmann*, 2009; *Li et al.*, 2012; *Jing et al.*, 2015]. Moreover, the wind stress curl-induced Ekman pumping is considered to be another crucial effect generating the coastal upwelling off eastern Hainan Island and eastern Leizhou Peninsula [*Jing et al.*, 2009]. Recently, the upwelling has been classified into three patterns, i.e., intensified upwelling off the eastern coast of Hainan Island (HEU), intensified upwelling off the northeastern coast of Hainan Island (HNEU), and both HEU and HNEU in 1 day [*Lin et al.*, 2016a]. Reanalysis data and satellite data have shown that the HEU is mainly driven by southwesterly wind and is not affected remarkably by fresh water, whereas the HNEU is associated with the prevailing southeasterly wind and can be limited in the lower layer when it is covered by fresh water. Numerical experiments have further indicated that the HNEU is principally intensified by an along-isobath barotropic pressure gradient force, but baroclinic processes make negative contributions to the formation of the HNEU [*Lin et al.*, 2016b].

2.2.4. Upwelling or Cold Dome Northeast of Taiwan Island

The cold eddy or upwelling off the northeastern part of Taiwan Island has been studied for several decades because the cyclonic eddy is regarded as an important conduit for the exchange of material between the ECS shelf and the adjoining Kuroshio [*Wong et al.*, 2000].

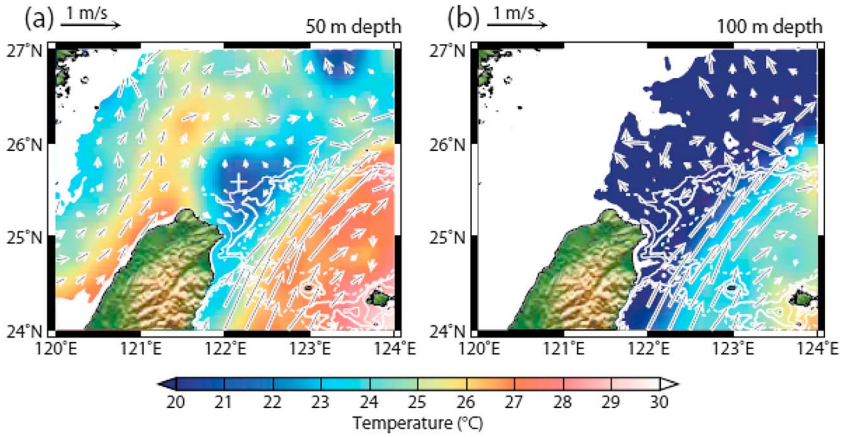

Figure 8. Climatological mean temperature and current velocity (arrows) in summer (May–September) at the depths of (a) 50 m and (b) 100 m. The 200 m (thin white line), 500 m (thick white line), and 1000 m (dashed white line) isobaths are plotted in each panel. The white cross in Figure 8a marks the center of the cold dome. Cited from Figure 2 of *Jan et al.* [2011].

Observational data have revealed the seasonal variation, three-dimensional structure, and spatial-temporal distribution of the cold eddy northeast of Taiwan [e.g., *Xiu et al.*, 2001; *Wang et al.*, 2008; *Chang et al.*, 2009]. The cold eddy exists northeast of Taiwan all year round, with two or three cold cores in summer and autumn, and has large seasonal variations. The cold eddy is characterized by low temperature, high salinity, high density, low dissolved oxygen, high phosphate, high silicate, and high nitrate [*Tseng et al.*, 2012]. These features are related to the dynamic balance between the Kuroshio meandering and the TWS water intruding into the ECS continental shelf. In particular, this cold eddy was also found to have atmospheric effects in spring and winter due to the intrusions of warm Kuroshio water onto the continental shelf of the ECS [*Chow et al.*, 2015].

Numerical modeling has also indicated that an upwelling is located in the shelf break off northeast Taiwan. Some model results have suggested that strong upwelling exists when the Kuroshio surface water intrudes from the sea area northeast of Taiwan to the continental shelf and that the largest upwelling speed is on the order of 5×10^{-6} m/s [e.g., *Lee and Chao*, 2003; *Xiu and Huang*, 2006; *Wu et al.*, 2008]. Another model proposed that vorticity effects are prominent in the upwelling in the nonsummer months [*Chang et al.*, 2010].

The cold eddy northeast of Taiwan has also been recognized as a cold dome that results in the formation of upwelling in the northeastern Taiwan shelf [e.g., *Jan et al.*, 2011] and has been confirmed by some high-resolution numerical models [e.g., *Gopalakrishnan et al.*, 2013]. The cold dome has a diameter of approximately 100 km, is centered around (25.625°N, 122.125°E) when taking the temperature at 50 m depth as the reference (Figure 8), and is maintained by cold and saline water upwelled along the continental slope. Monsoon-driven intrusion of the Kuroshio onto the ECS shelf intensifies the upwelling and brings more subsurface water up to the cold dome during winter than during summer monsoon season. However, it is suggested that the surface cold dome occurs more frequently in summer, when it includes an unusual contribution from the cold water residual associated with typhoon events [*Shen et al.*, 2011].

2.2.5. Biogeochemical Responses to Upwelling

As upwelling is a key driver of biogeochemical processes and ecosystem dynamics, the biogeochemical responses to upwelling in the China seas have been considered to be of importance for decades. For example, multiple satellite data have shown that the Vietnam coastal upwelling coincides with the regional increase of phytoplankton biomass in terms of shape, timing, and location [e.g., *Tang et al.*, 2004b].

The northeasterly monsoon wind-induced upwelling has important effects on the biogeochemical cycles in the Luzon cold eddy region [e.g., *Chen et al.*, 2006]. Specifically, in the region northwest of Luzon Island, the winter phytoplankton bloom is primarily induced by Ekman pumping-driven upwelling (observed at about 50 m below the sea surface) and upper mixed layer entrainment [e.g., *J. J. Wang et al.*, 2010; *Zhao et al.*, 2012]. In the Luzon Strait, the winter bloom occurs during the relaxation period of intensified northeasterly winds when the deepened mixed layer starts to shoal, and the advection of relative vorticity primarily contributes to the subsurface upwelling that supplies nutrients to the region below the mixed layer [*Lu et al.*,

2015]. In the Sabah waters of the southeastern SCS, phytoplankton blooms frequently appear from December to the following April as a result of strong northeasterly wind-induced coastal upwelling [*Abdul-Hadi et al*., 2013].

Upwelling in the ECS, the Yellow Sea, and the Bohai Sea can also be verified by the distribution of marine chemical and biological elements [*Chen et al*., 2004; *Wong et al*., 2004]. Observations in the 2000s showed that the spring upwelling increases the phosphate, nitrate, and silicate concentrations in the mixed layer, followed by an increase in Chl *a* concentration, but the summer upwelling is relatively weaker and is strongly influenced by turbid Yangtze River plume water [*Pei et al*., 2009; *Wei et al*., 2011]. The Yangtze River plume water and coastal upwelling can significantly influence the horizontal and vertical heterogeneities of phytoplankton phosphorus deficiency in the Yangtze River plume [*Tseng et al*., 2014].

Coupled physical and biological models have been applied to study upwelling and its associated biogeochemical responses in the Bohai Sea [*Zhang et al*., 2002; *Wang et al*., 2007]. Another coupled physical-biological numerical ocean model estimated the physical (i.e., coastal upwelling) and biological effects on nutrient transport in the TWS during summer [*J. Wang et al*., 2013]. These results indicated that high phytoplankton biomass appears in the upwelling region.

Many studies have focused on the responses of phytoplankton to typhoon-induced upwelling [e.g., *Zheng and Tang*, 2007; *Chang et al*., 2008; *Zhao et al*., 2013]. If the typhoon has a longer forcing time, it may induce a stronger phytoplankton bloom. Chl *a* concentration (>3 mg/m^3) in the SCS is 30 times larger after typhoon passage in comparison with the respective monthly mean level of Chl *a* concentration [*Chen et al*., 2012]. This kind of typhoon-induced bloom often appears along or to the right of the typhoon track a few days after the passage of the typhoon and lasts for 1–2 weeks at the surface layer or even more than 3 weeks in the subsurface layer [*Ye et al*., 2013]. Moreover, the ocean-atmosphere interactions and fisheries data collected before and after the passage of several typhoons across the southern region of the ECS suggested that typhoons can enhance upwelling that results not only in increases of Chl *a* but also in changes of local fish communities and, consequently, fishing activities [*Chang et al*., 2014]. Typhoon-induced upwelling can indeed stimulate efficient particulate organic carbon export out of the euphotic zone [*Shih et al*., 2013]. In the waters near the typhoon's path, especially in the typhoon-induced upwelling area, nutrient-rich bottom water stirred by the typhoon can promote an outbreak of aquatic organisms and significantly increase the probability of red tide occurrence [*Li et al*., 2015].

2.3. Summary

There are 12 major upwelling regions in the China seas, as shown in Figure 2. Some principal features of these upwelling regions are summarized below.

1. The summertime upwelling regions in the northern SCS are mostly along the eastern coast of Hainan Island and along the coasts of eastern Guangdong and southern Fujian.
2. Coastal upwelling in the western SCS usually appears along the Vietnam coast in summer, with the strongest intensity in August being accompanied by a cold jet extending eastward from the coastal waters. The Vietnam cold eddy is located east of the central Vietnam coast.
3. The Luzon cold eddy is a large eddy off western Luzon Island in winter.
4. Four upwelling regions in the TWS are located along the southwestern and northwestern coasts of the TWS, around the Taiwan Bank, and around the Penghu Islands.
5. Coastal upwelling exists in the Yangtze River Estuary and along the Zhejiang coast in the ECS. In addition, an upwelling or a cold dome also appears in the outer shelf break area of the ECS, i.e., in the sea area off northeastern Taiwan Island.
6. Additionally, four other upwelling regions in the China seas (Figure 2) have been reported to sometimes appear in the northern Bohai Strait [*Wei et al*., 2003], off the southwest coast of Hainan Island [*Lü et al*., 2008], along the east coast of Peninsular Malaysia [*Daryabor et al*., 2014], and near the Sabah coast of the southeastern SCS [*Abdul-Hadi et al*., 2013], respectively.

3. Upwelling Dynamics With Applications to the China Seas

Although many numerical models have been applied to study the upwelling dynamics, there still exist diverging views for interpreting each upwelling region in the China seas. Upwelling is an oceanographic

Table 1. Principal Mechanisms or Influent Factors for the Major Upwelling Regions in the China Seas

Upwelling Region or Type	Alongshore Wind	Wind Stress Curl	Widened Shelf or Shelf Break	Cape or Canyon	Tidal Mixing or Internal Tides	Stratification	Background Flow
East of Guangdong	a		b		b	b	b
East of Hainan	a	b					
East of Vietnam	a						
Vietnam cold eddy		a					b
West of Luzon Island	b	a					b
Southwestern Taiwan Strait	a						b
Northwestern Taiwan Strait	a			b			b
Around Taiwan Bank			a		b		b
Around Penghu Islands				b			a
East of Zhejiang	a		b	b	b		b
Off Yangtze River Estuary	a			b		b	
Northeast of Taiwan		b	a				b
Northern Bohai Strait							a
Southwest of Hainan					a		
East of Peninsular Malaysia	a						
Near Sabah coast	a						
Cyclone-induced upwelling		a					b

[a]Primary factor.
[b]Secondary or contributing factor.

phenomenon that involves motion of dense, cooler, and usually nutrient-rich water toward the ocean surface. Therefore, upwelling process is associated with horizontal and vertical variations of cross-isobath transport, which follows the vertically integrated momentum equations (see Appendix A). Under some assumptions, the momentum equations may be transformed to different forms, which can accordingly examine various contributing factors for upwelling.

Generally speaking, according to the momentum equations, the principal mechanisms for generating the upwelling include the alongshore wind and wind stress curl, which are controlling factors of upwelling dynamics. Topography, such as widened shelf, shelf break, cape, or canyon (or submerged valley), also has a significant role in modulating the upwelling. In addition, tide (tidal mixing or internal tide), stratification, and background flow are important factors affecting the upwelling. However, one may adopt a different upwelling dynamics by *Liang and Robinson* [2009], which provided a real ocean example of how secondary upwelling can be driven by winds through nonlinear instability and of how winds may excite the ocean following a process markedly different from the classical explanation. Here we summarize seven important factors associated with the upwelling mechanism, mostly for the China seas and also for global upwelling regions.

3.1. Wind: Alongshore Wind

According to the classical Ekman transport theory, alongshore wind causes cross-shore transport of an upper water volume and thus induces coastal upwelling or downwelling along the coast. The southwesterly monsoon winds prevail along the eastern coasts of Vietnam, Peninsular Malaysia, Hainan, Guangdong, Fujian (or the southwestern and northwestern TWS), and Zhejiang in summer [e.g., *Dippner et al*., 2007; *Qiao and Lü*, 2008; *Wang et al*., 2012], whereas the northeasterly monsoon winds are almost along the western coast of Luzon Island and along the Sabah coast (or off northwest Borneo) in winter [e.g., *Yan et al*., 2015]. Therefore, the wind-driven offshore Ekman transport becomes a vital mechanism for the coastal upwelling along these coasts of the China seas in summer or in winter (Table 1). However, the coastal upwelling along the eastern Guangdong coast may still exist even when the upwelling-favorable southwesterly wind retreats because the topographically induced upwelling is comparable with the wind-driven upwelling at surface and has a stronger contribution to the upwelling intensity than the local wind does at bottom in the nearshore shelf region of the northern SCS [*Shu et al*., 2011; *Wang et al*., 2014].

3.2. Wind: Wind Stress Curl

In the open ocean, a cyclonic wind field generates a cyclonic circulation, which induces upwelling due to Ekman pumping. The Ekman pumping velocity w_H that results from convergence or divergence in the

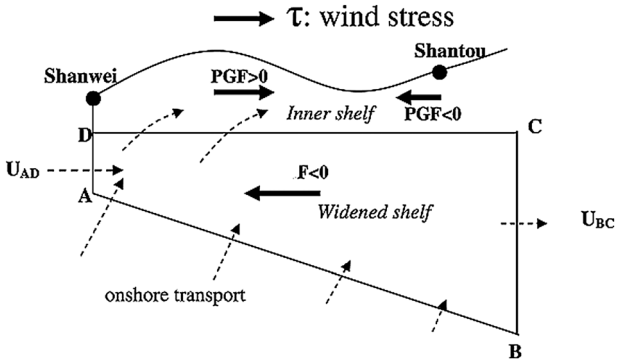

Figure 9. Schematic showing the wind-driven upwelling processes and the forcing mechanism over the middle and inner shelves of a widened shelf in the northern SCS. Cited from Figure 10 of *Gan et al.* [2009a]. PGF denotes pressure gradient force; U_{AD} and U_{BC} are mean velocities normal to the line *AD* at the head of the widened shelf (near Shanwei) and the line *BC* downstream of it (near Shantou), respectively.

Ekman layer is derived by integrating the mass conservation equation over the Ekman layer [*Chereskin and Price*, 2001]:

$$w_H = \frac{\partial(\tau_0^y/\rho f)}{\partial x} - \frac{\partial(\tau_0^x/\rho f)}{\partial y}$$

where ρ is the density of seawater, f is the Coriolis parameter, and τ_0^x and τ_0^y are the eastward and northward wind components, respectively. Thus, the Ekman pumping is given by the spatial derivative or curl of the wind stress (divided by ρf). For this reason, a tropical cyclone or a wind field with positive wind stress curl (in the Northern Hemisphere) can induce an evident upwelling off the coast or in the open ocean. For the eastern boundary upwelling systems, such as in the Peru upwelling system and the California upwelling system, wind stress curl-induced upwelling has been found to be significant only in offshore regions, whereas coastal upwelling better represents the dynamics of inshore areas [*Albert et al.*, 2010; *Macías et al.*, 2012]. Similarly, wind stress curl plays an important role in generating the Vietnam cold eddy [*Xie et al.*, 2003; *D. K. Wang et al.*, 2013], the Luzon cold eddy [*Liao et al.*, 2008], and the tropical cyclone-induced upwelling in the China seas (Table 1). Meanwhile, cyclonic wind curls behind a coastal mountain range, or orographically induced cyclonic wind curls, are also a factor for the Vietnam cold eddy, the Luzon cold eddy, or the cold dome northeast of Taiwan [e.g., *Xie et al.*, 2003].

3.3. Topography: Widened Shelf or Shelf Break

As shown in Figure 9, the northern SCS has a distinctly eastward widened shelf between Shanwei and Shantou (i.e., east of Guangdong). When southwesterly wind blows along the coast, a positive pressure gradient force (PGF in the figure) upstream near Shanwei and a negative PGF downstream of the coastal cape near Shantou over the inner shelf are chiefly induced by the formation of higher pressure at the shoreward convex coastline. Meanwhile, with mass conservation (i.e., $u_{BC}\ S_{BC} = u_{AD}\ S_{AD}$ in the figure), $\boldsymbol{F} = \rho u_{BC}\ S_{BC}(u_{BC} - u_{AD})$, in which S_{AD} and S_{BC} are the areas at the cross sections along two streamlines *AD* and *BC*, respectively. Since $u_{AD} > u_{BC}$, a net westward force, $\boldsymbol{F} < 0$, is formed over the widened shelf as a result of the net rate of momentum influx within the water volume bounded with the lines *AB* and *CD* (Figure 9) [*Gan et al.*, 2009a]. This net westward force produces a shoreward transport. Therefore, the cold dense water, advected from upstream near the head of the widened shelf, outcrops at the lee of the coastal cape near Shantou and thus intensifies the coastal upwelling there [*Gan et al.*, 2009a]. In addition, the along-isobath pressure gradient force can also be generated by net bottom stress curl primarily associated with the shear vorticity field induced by coastal jet over the shelf with variable shelf topography such as a widened shelf [*Gan et al.*, 2013].

Upwelling at a shelf break can be caused by the buoyancy shutdown, a process by which reduced bottom stress weakens the offshore Ekman transport [*Benthuysen et al.*, 2015]. Over the shelf, an offshore bottom Ekman transport develops at the bottom boundary layer of the shelf within an inertial period, whereas over the slope, downslope buoyancy advection tilts isopycnals downward over a bottom boundary layer depth ($\mathbf{h_{BBL}}$ in Figure 10) and bottom cross-shelf transport is weakened due to the reduced near-bottom speed and the thickening bottom boundary layer. Then, the convergence in the bottom transport induces adiabatic upwelling offshore of the shelf break (Figure 10). A similar approach can be applied to some upwelling regions in the China seas, such as southeast of the Taiwan Bank or in the shelf break of the ECS (Table 1), to further reveal the upwelling dynamics there.

3.4. Topography: Cape or Canyon

Cape or canyon topography is often seen along the coast of the China seas due to the winding coastline and rough bottom topography; thus, the coastal upwelling can be affected remarkably by a cape or a canyon

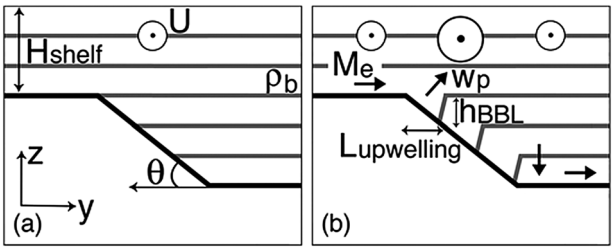

Figure 10. Flow adjustment. (a) At initial time, the initial density field ρ_b (gray lines) is linearly stratified. (b) After an inertial period, the bottom cross-shelf transport converges over the shelf break and leads to upwelling $\mathbf{w_p}$ out of the boundary layer. **U** is alongshore flow, $\mathbf{H_{shelf}}$ is depth of the shelf, $\mathbf{M_e}$ is offshore bottom Ekman transport, $\mathbf{h_{BBL}}$ is bottom boundary layer depth, and $\mathbf{L_{upwelling}}$ is the horizontal length scale of upwelling. Cited from Figure 1 of *Benthuysen et al.* [2015].

(Table 1). When a cyclonic current flows around a cape, the relative vorticity change along a streamline is favorable and dominant for producing an upwelling downstream and adjacent to the cape, whereas the frictional diffusion of vorticity has a lower or even opposite effect. The relative vorticity change overwhelms the frictional diffusion of vorticity for determining vertical velocity at 20–27 km offshore [*Z. Y. Chen et al.*, 2014]. As for a coastal canyon, upwelling is produced over the canyon axis and in the downstream area of the canyon by the relative vorticity change, while the frictional diffusion of vorticity causes only positive (negative) smaller vertical velocity upstream (downstream) of the canyon. Therefore, relative vorticity change becomes a dominant upwelling mechanism downstream of a cape or a canyon in the northwestern TWS where one of these features occurs off Pingtan Island or Sansha Bay [*Z. Y. Chen et al.*, 2014]. As shown schematically in Figure 11, if a surface flow passes over a canyon, near-surface isopycnals may be elevated and a cyclonic eddy ("Rim Depth Eddy" in the figure) is thus generated. Then, flow over the slope at the depth of the canyon rim and for some depth below ("Upwelling Current" in the figure) is advected into the canyon and upwells over the downstream rim of the canyon near the head. This flow carries the deeper water advected onto the shelf [*Allen and Hickey*, 2010].

Another mechanism inducing upwelling near a coastal promontory or a cape, just like the one over the ECS shelf, is the strengthened geostrophic shoreward transport downstream of a promontory due to the formation of a countercurrent (negative) pressure gradient force around the promontory as the upwelling jet veers shoreward [*Liu and Gan*, 2014]. However, the pressure gradient force that drives the upwelling over a submerged valley in the ECS is the combined result of the nonlinearity due to vertical squeezing of vortex tube and bottom frictional effects [*Liu and Gan*, 2015].

3.5. Tidal Mixing or Internal Tide

Tide, through a tidal mixing effect or internal tide, plays a key role in modulating or intensifying the upwelling, such as around the Taiwan Bank or southwest of Hainan Island (Table 1). For the upwelling around the Taiwan Bank, upward transport of the SCS water carries cold water from the subsurface layer to a depth of approximately 25 m near the Taiwan Bank, then strong tidal mixing forces this upwelled water further upward to the surface or near the surface layer [*Hong et al.*, 2011a; *Jiang et al.*, 2011]. For the summertime upwelling off the southwestern coast of Hainan Island, the existing tidal mixing front [*Hu et al.*, 2003a] has been identified as a vital factor triggering the upwelling [*Lü et al.*, 2008]. In addition, tides contribute to the generation of the upwelling off the Yangtze River Estuary because tidal mixing facilitates the expansion of the Yangtze River plume water [*Qiao et al.*, 2006], and strong tidal mixing results in a considerable horizontal density gradient across a tidal front and thus induces upwelling [*Lü et al.*, 2006, 2007]. Another research has shown that strong tidal mixing plays a dominant role in the formation of the upwelling around the Yellow Sea Cold Water Mass [*Lü et al.*, 2010].

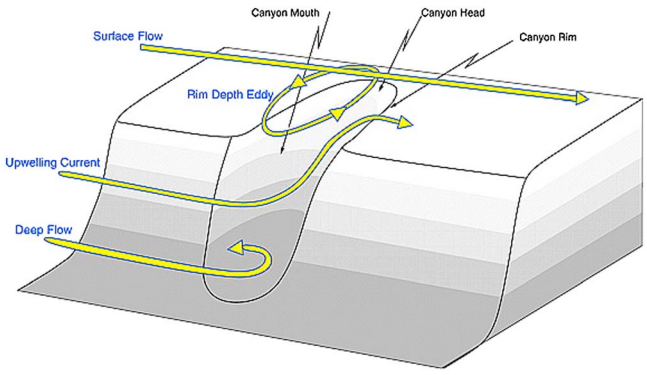

Figure 11. Schematic of the advection-driven flow over a submarine canyon. Cited from Figure 1 of *Allen and Hickey* [2010].

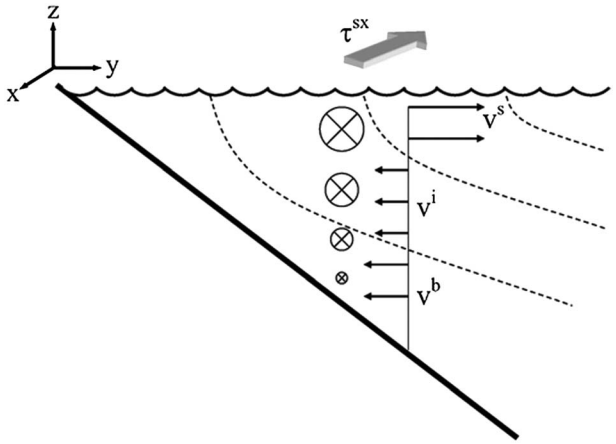

Figure 12. Schematic of the cross-shelf flow and isopycnals in response to an upwelling-favorable wind stress. τ^{SX} is along-shelf wind stress, $\mathbf{V^s}$ is wind-driven offshore flow in the surface boundary layer, and $\mathbf{V^i}$ and $\mathbf{V^b}$ are onshore flows in the interior and bottom boundary layers, respectively. Cited from Figure 2 of *Lentz and Chapman* [2004].

Meanwhile, internal tides can affect the upwelling, especially in the southern Taiwan Bank, off the coast of eastern Guangdong, and in the northern SCS, where internal tides can enhance the uplifting of lower layer water and thus intensify the upwelling [*Gu et al*., 2012; *Pan et al*., 2012a]. Therefore, the summertime upwelling pattern and intensity tend to be altered on the shelf off Guangdong as a result of the interaction between the upwelling and internal tides.

3.6. Stratification

Stratified fluid occurs regularly in the China seas in summer or in the coastal area when it is affected by the river plume. The buoyancy in the plume alters the wind-driven upwelling circulation by thinning and strengthening both the seaward transport in the plume and the shoreward transport beneath it [*Gan et al*., 2009b]. Stratification has a profound influence on the wind-driven upwelling or downwelling over a shallow shelf. When the water column is stratified, the wind-driven near-surface cross-shelf transport has similar magnitude but opposite direction as the near-bottom cross-shelf transport over the mid and outer shelf. Under the stratified condition, upwelling or downwelling is usually confined near the coast where stratification may be maintained by a balance between vertical mixing and buoyancy forcing [*Lentz*, 2001]. Given a two-dimensional, wind-driven, and stratified flow over a sloping bottom (Figure 12), the geostrophic along-shelf flow is in the direction of the wind stress and decreases linearly with depth. Therefore, an upwelling is generated by the wind-driven offshore transport in the surface boundary layer, which is balanced by the friction-driven onshore transport in the bottom boundary layer over the shelf [*Lentz and Chapman*, 2004].

For a stratified fluid, the Joint Effect of Baroclinicity and Relief (JEBAR) term in the momentum equations also plays an important role in upwelling or downwelling phenomena. Such situations are usually typical for the upwelling or downwelling off the Pearl River Estuary in the northern SCS [*Gan et al*., 2013] (Table 1).

3.7. Background Flow

Background flow, such as the Kuroshio, local circulation, eddy, or near-bottom current, is another factor affecting or modulating the upwelling. This influencing factor has been recognized frequently in the China seas (Table 1). For example, as long as there exists an alongshore eastward current, no matter the case of upwelling/upwelling relaxation or downwelling relaxation/downwelling, it activates the interaction of the flow with the widened shelf topography to form shoreward geostrophic and bottom Ekman transports, from which a cross-isobath shoreward upslope motion is formed [*Gan et al*., 2015]. In the ECS, the Taiwan Warm Current itself is a producer for the coastal upwelling through its encroachment and ascending onto the topography slope, especially in summer [*Lü et al*., 2006], but the Taiwan Warm Current may weaken the upwelling in winter [*Qiao et al*., 2006].

Additionally, the mesoscale warm eddies produced by the Kuroshio intrusion into the ECS have remarkable effects on modulating upwelling [*Xiu et al*., 2002]. It is therefore significant to pursue further understanding of how these eddies or currents (i.e., the Kuroshio) interact with upwelling, especially in the SCS and the ECS, where mesoscale eddies are mostly active [e.g., *Li et al*., 2003].

4. Some Considerations on Further Upwelling-Related Studies

This paper reviewed the studies of upwelling in the China seas, namely, the SCS, the TWS, the ECS, the Yellow Sea, and the Bohai Sea, conducted since 2000. The upwelling in the coastal waters of China is complex. It is

characterized not only by long-term variation associated with ENSO events and global climate change but also by short-term variation related to winds, internal tides, and tropical cyclones. Therefore, it is difficult to rely on observations by limited cruises or at several stations to reveal the dynamic and biogeochemical processes in these upwelling regions. It has been suggested that long-term monitoring be implemented to investigate the upwelling and its surrounding dynamic environments using satellite technology and seabed-based and shore-based observations [*Hu et al*., 2003b]. During 2005–2011, offshore surveys were conducted in all four seasons to obtain comprehensive observational data in the Chinese coastal waters. These data, combined with multisource satellite data and marine eco-dynamic models, have resulted in a deepened understanding of the upwelling and its dynamic environments in the coastal waters of China [*Qiao*, 2012; *Xiong et al*., 2012].

The following aspects should be addressed in future upwelling studies in the China seas.

1. *Potential intensification of coastal upwelling under global climate change*. An intensification of coastal upwellings in response to global climate change has been proposed through the last few decades [e.g., *Bakun*, 1990; *McGregor et al*., 2007]. A similar trend also exists in the China seas. For instance, the wind-driven coastal upwelling off eastern Hainan, Guangdong, and Zhejiang has shown a trend of intensification based on 40 year coastal upwelling index [*Bakun*, 1973] data [*Miao and Hu*, 2011]. A state-space decomposition of the alongshore wind stress time series exhibited an intensification of upwelling in the SCS during the "upwelling season" for the period of 1988–2008 [*Su et al*., 2013]. Climate change effects on regional monsoon are complex and uncertain. Specifically, changes in the large-scale Asian summer monsoon [*Christensen et al*., 2013] will certainly affect coastal winds and upwelling. Clearly, more research should be conducted to reveal the response of coastal upwelling to global climate change, for the upwelling in the China seas and also for global upwelling regions.
2. *Downwelling study*. Compared with upwelling, it is more difficult to describe downwelling by means of temperature and salinity distributions. Recent observational, theoretical, and modeling studies have suggested that downwelling results from surface buoyancy loss in boundary currents or is concentrated in strong currents subject to buoyancy loss near lateral boundaries [e.g., *Spall*, 2008; *Cenedese*, 2012]. For the China seas, the dynamics of intensified downwelling over a widened shelf in the northeastern SCS have been studied [*Gan et al*., 2013], and this study may be regarded as a pioneer work for stimulating more downwelling studies in the China seas. Since the trend of global warming became prominent, a number of papers have focused on carbon sequestration, deep-sea cycling mechanisms, and especially on the downwelling that transports carbon downward to the deep ocean. Therefore, the study of downwelling should be pushed forward.
3. *Intrusion of upwelling into a coastal embayment*. Upwelling-related cold water has been reported to intrude Sanya Bay (located south of Hainan Island) [*Dong et al*., 2002]. Coastal upwelling of oxygen-depleted bottom water was observed intruding Tokyo Bay, which caused mortality of shellfish and other aquatic animals around the bay [*Zhu and Yu*, 2014]. The behavior of the bottom water intruded into a bay varies with wind direction and strength. Because there are many small embayments along the coastlines of the China seas, a systematic study of upwelling intrusion into the bays and estuaries of the China seas will be of significance, both scientifically and ecologically, to these coastal environments.
4. *Influence of upwelling on fishery and biogeochemical processes*. This paper reviewed the upwelling in the China seas, mostly in term of its hydrographic features. However, upwelling has a great impact on biogeochemical and even fisheries-related processes, which are the well-known elements usually associated with upwelling systems. For example, upwelling can exert significant influences on biological activities in the euphotic zone, where light can penetrate, and can also impact particulate organic carbon export flux depending on upwelling conditions [*Jiao et al*., 2014]. This topic deserves a follow-up review in the near future in cooperation with other scientists in the fields of biogeochemistry and fisheries.

Appendix A

Upwelling process is associated with horizontal and vertical variations of cross-isobath transport, which follows the vertically integrated momentum equations transformed to a rotating coordinate system, in which p and n indicate the along-isobath and cross-isobath directions, respectively [*Lin et al*., 2016b]:

$$\overbrace{\frac{\partial}{\partial t}\int_{-h_2}^{-h_1} v^p \mathrm{d}z}^{\text{ACC}} + \overbrace{\frac{\partial}{\partial n}\int_{-h_2}^{-h_1} u^n v^p \mathrm{d}z + \frac{\partial}{\partial p}\int_{-h_2}^{-h_1} v^p v^p \mathrm{d}z}^{\text{GMF}} + \overbrace{f\int_{-h_2}^{-h_1} u^n \mathrm{d}z}^{\text{Coriolis force}}$$
$$= \overbrace{-\frac{\partial \chi}{\partial p} - \frac{g}{\rho_0}\left(\frac{\partial h_1}{\partial p}\int_{-h_1}^{0}\rho \mathrm{d}z' - \frac{\partial h_2}{\partial p}\int_{-h_2}^{0}\rho \mathrm{d}z'\right)}^{\text{PGC}} + \overbrace{\int_{-h_2}^{-h_1}\left(-g\frac{\partial \zeta}{\partial p} + K_h\nabla^2 v^p + \frac{\tau^p}{\rho_0}\right)}^{\text{PGT}}{}^{\text{HVI}}{}^{\text{VVI}} \mathrm{d}z, \tag{A1}$$

$$\frac{\partial}{\partial t}\int_{-h_2}^{-h_1} u^n \mathrm{d}z + \frac{\partial}{\partial n}\int_{-h_2}^{-h_1} u^n u^n \mathrm{d}z + \frac{\partial}{\partial p}\int_{-h_2}^{-h_1} u^n v^p \mathrm{d}z - f\int_{-h_2}^{-h_1} v^p \mathrm{d}z$$
$$= -\frac{\partial \chi}{\partial n} - \frac{g}{\rho_0}\left(\frac{\partial h_1}{\partial n}\int_{-h_1}^{0}\rho \mathrm{d}z' - \frac{\partial h_2}{\partial n}\int_{-h_2}^{0}\rho \mathrm{d}z'\right) \tag{A2}$$
$$+\int_{-h_2}^{-h_1}\left(-g\frac{\partial \zeta}{\partial n} + K_h\nabla^2 u^n + \frac{\tau^n}{\rho_0}\right)\mathrm{d}z,$$

where

$$\chi = \frac{g}{\rho_0}\int_{-h_2}^{-h_1}\left(\int_{-z}^{0}\rho \mathrm{d}z'\right)\mathrm{d}z, \tag{A3}$$

In equations A1, A2, A3, ζ is the sea surface elevation, and the depths $-h_1$ and $-h_2$ are the upper and lower limits of the vertical integral, respectively. The terms on the left-hand side of equation (A1) are the along-isobath acceleration (ACC in the equation) of the along-isobath transport, the gradient of cross-isobath and along-isobath nonlinear momentum flux (GMF), and the Coriolis force. On the right-hand side, the baroclinic pressure gradient force (PGC) consists of three terms: the term with χ is related to the Joint Effect of Baroclinicity and Relief (referred to as JEBAR), and it is determined by both the topographic gradient and the horizontal density gradient [*D. X. Wang et al.*, 2010]. The other two terms represent the interaction between bottom pressure gradient force and topography. The barotropic pressure gradient force (PGT; the fourth term) depends only on the sea surface slope. The fifth term is the horizontal viscosity (HVI), and the last term is the vertical viscosity (VVI) associated with wind stress (τ) [*Lin et al.*, 2016b].

Acknowledgments

The authors appreciate the permissions from copyright holders to use several previously published figures in this review paper. Only the SST and wind data used to generate Figure 1 were provided by the NOAA/OAR/ESRL PSD, Boulder, Colorado, USA, from their website (http://www.esrl.noaa.gov/psd/). This review was supported jointly by the National Basic Research Program of China (2015CB954004) and the NSFC (U1405233 and 41276006). Hu finalized this review during his visit at the UNSW under a fellowship of the China Scholarship Council. This is publication No. 21 of the Sino-Australian Research Centre for Coastal Management. We are grateful to the Editor, Associate Editor, and three anonymous reviewers for their valuable suggestions and detailed comments for improving the manuscript. We also thank J. Zhu for redrawing some figures in the paper, Y.X. Wang for creating Figure 1, J.P. Gan for beneficial discussion, and Z.J. Yu for excellent editorial assistance in the English language.

References

Abdul-Hadi, A., S. Mansor, B. Pradhan, and C. K. Tan (2013), Seasonal variability of chlorophyll-*a* and oceanographic conditions in Sabah waters in relation to Asian monsoon—A remote sensing study, *Environ. Monit. Assess.*, *185*(5), 3977–3991.

Albert, A., V. Echevin, M. Lévy, and O. Aumont (2010), Impact of nearshore wind stress curl on coastal circulation and primary productivity in the Peru upwelling system, *J. Geophys. Res.*, *115*, C12033, doi:10.1029/2010JC006569.

Allen, S. E., and B. M. Hickey (2010), Dynamics of advection-driven upwelling over a shelf break submarine canyon, *J. Geophys. Res.*, *115*, C08018, doi:10.1029/2009JC005731.

Bakun, A. (1973), Coastal upwelling indices, west coast of North America, 1946–71, NOAA Tech. Rep. NMFS SSRF-671, U.S. Dep. of Commer.

Bakun, A. (1990), Global climate change and intensification of coastal ocean upwelling, *Science*, *247*(4939), 198–201.

Barthel, K., R. Rosland, and N. C. Thai (2009), Modelling the circulation on the continental shelf of the province Khanh Hoa in Vietnam, *J. Mar. Syst.*, *77*(1–2), 89–113.

Benthuysen, J., L. N. Thomas, and S. J. Lentz (2015), Rapid generation of upwelling at a shelf break caused by buoyancy shutdown, *J. Phys. Oceanogr.*, *45*(1), 294–312.

Boyer, T., S. Levitus, H. Garcia, R. Locarnini, C. Stephens, and J. Antonov (2005), Objective analyses of annual, seasonal, and monthly temperature and salinity for the world ocean on a 0.25° grid, *Int. J. Climatol.*, *25*(7), 931–945.

Cenedese, C. (2012), Downwelling in basins subject to buoyancy loss, *J. Phys. Oceanogr.*, *42*(11), 1817–1833.

Chang, Y., H.-T. Liao, M.-A. Lee, J.-W. Chan, W.-J. Shieh, K.-T. Lee, G.-H. Wang, and Y.-C. Lan (2008), Multisatellite observation on upwelling after the passage of Typhoon Hai-Tang in the southern East China Sea, *Geophys. Res. Lett.*, *35*, L03612, doi:10.1029/2007GL032858.

Chang, Y., J. W. Chan, Y. C. A. Huang, W. Q. Lin, M. A. Lee, K. T. Lee, C. H. Liao, K. Y. Wang, and Y. C. Kuo (2014), Typhoon-enhanced upwelling and its influence on fishing activities in the southern East China Sea, *Int. J. Remote Sens.*, *35*(17), 6561–6572.

Chang, Y.-L., C.-R. Wu, and L.-Y. Oey (2009), Bimodal behavior of the seasonal upwelling off the northeastern coast of Taiwan, *J. Geophys. Res.*, *114*, C03027, doi:10.1029/2008JC005131.

Chang, Y.-L., L.-Y. Oey, C.-R. Wu, and H.-F. Lu (2010), Why are there upwellings on the northern shelf of Taiwan under northeasterly winds?, *J. Phys. Oceanogr.*, *40*(6), 1405–1417.

Chen, C. C., F. K. Shiah, S. W. Chung, and K. K. Liu (2006), Winter phytoplankton blooms in the shallow mixed layer of the South China Sea enhanced by upwelling, *J. Mar. Syst.*, *59*(1–2), 97–110.

Chen, C. T. A., C.-T. Liu, W. S. Chuang, Y. J. Yang, F.-K. Shiah, T. Y. Tang, and S. W. Chung (2003), Enhanced buoyancy and hence upwelling of subsurface Kuroshio waters after a typhoon in the southern East China Sea, *J. Mar. Syst.*, *42*(1–2), 65–79.

Chen, D. K., X. T. Lei, W. Wang, G. H. Wang, G. J. Han, and L. Zhou (2013), Upper ocean response and feedback mechanisms to typhoon [in Chinese with English abstract], *Adv. Earth Sci.*, *28*(10), 1077–1086.

Chen, J. Q., Z. L. Fu, and F. X. Li (1982), A study on upwelling in Minnan–Taiwan Shoal fishing ground [in Chinese with English abstract], *Taiwan Strait*, *1*(2), 5–13.

Chen, X. Y., D. L. Pan, X. Q. He, Y. Bai, and D. F. Wang (2012), Upper ocean responses to category 5 typhoon Megi in the western North Pacific, *Acta Oceanol. Sin.*, *31*(1), 51–58.
Chen, X. Y., Z. Z. Hao, D. L. Pan, S. X. Huang, F. Gong, and D. S. Shi (2014), Analysis of temporal and spatial feature of sea surface wind filed in China offshore [in Chinese with English abstract], *J. Mar. Sci.*, *32*(1), 1–10.
Chen, Y. L. L., H. Y. Chen, G. C. Gong, Y. H. Lin, S. Jan, and M. Takahashi (2004), Phytoplankton production during a summer coastal upwelling in the East China Sea, *Cont. Shelf Res.*, *24*(12), 1321–1338.
Chen, Z. Y., X.-H. Yan, and Y. W. Jiang (2014), Coastal cape and canyon effects on wind-driven upwelling in northern Taiwan Strait, *J. Geophys. Res. Oceans*, *119*, 4605–4625, doi:10.1002/2014JC009831.
Chereskin, T. K., and J. F. Price (2001), Ekman transport and pumping, in *Encyclopedia of Ocean Sciences*, vol .2, pp. 809–815, Elsevier.
Chiang, T.-L., C.-R. Wu, and L.-Y. Oey (2011), Typhoon Kai-Tak: An ocean's perfect storm, *J. Phys. Oceanogr.*, *41*(1), 221–233.
Chow, C. H., Q. Y. Liu, and S.-P. Xie (2015), Effects of Kuroshio intrusions on the atmosphere northeast of Taiwan Island, *Geophys. Res. Lett.*, *42*, 1465–1470, doi:10.1002/2014GL062796.
Christensen, J. H., et al. (2013), Climate phenomena and their relevance for future regional climate change, in *Climate Change 2013: The Physical Science Basis. Contribution of Working Group I to the Fifth Assessment Report of the Intergovernmental Panel on Climate Change*, edited by T. F. Stocker et al., pp. 1217–1308, Cambridge Univ. Press, Cambridge, U. K.
Chu, P. C., J. M. Veneziano, C. W. Fan, M. J. Carron, and W. T. Liu (2000), Response of the South China Sea to tropical cyclone Ernie 1996, *J. Geophys. Res.*, *105*, 13,991–14,009, doi:10.1029/2000JC900035.
Cui, H., S. W. Zhang, and Q. Y. Wang (2009), Numerical calculation of the response of the South China Sea to Typhoon Imbudo [in Chinese with English abstract], *Acta Phys. Sin.*, *58*(9), 6609–6615.
Daryabor, F., F. Tangang, and L. Juneng (2014), Simulation of southwest monsoon current circulation and temperature in the east coast of Peninsular Malaysia, *Sains Malays.*, *43*(3), 389–398.
Dippner, J. W., and N. Loick-Wilde (2011), A redefinition of water masses in the Vietnamese upwelling area, *J. Mar. Syst.*, *84*(1–2), 42–47.
Dippner, J. W., K. V. Nguyen, H. Hein, T. Ohde, and N. Loick (2007), Monsoon-induced upwelling off the Vietnamese coast, *Ocean Dyn.*, *57*(1), 46–62.
Dong, J. D., H. K. Wang, S. Zhang, and L. M. Huang (2002), Vertical distribution characteristics of seawater temperature and DIN in Sanya Bay [in Chinese with English abstract], *J. Trop. Oceanogr.*, *21*(1), 40–47.
Fang, W. D., G. H. Fang, P. Shi, Q. Z. Huang, and Q. Xie (2002), Seasonal structures of upper layer circulation in the southern South China Sea from in situ observations, *J. Geophys. Res.*, *107*(C11), 3202, doi:10.1029/2002JC001343.
Gan, J., H. Li, E. N. Curchitser, and D. B. Haidvogel (2006), Modeling South China Sea circulation: Response to seasonal forcing regimes, *J. Geophys. Res.*, *111*, C06034, doi:10.1029/2005JC003298.
Gan, J. P., and T. D. Qu (2008), Coastal jet separation and associated flow variability in the southwest South China Sea, *Deep Sea Res., Part I*, *55*(1), 1–19.
Gan, J. P., A. Cheung, X. G. Guo, and L. Li (2009a), Intensified upwelling over a widened shelf in the northeastern South China Sea, *J. Geophys. Res.*, *114*, C09019, doi:10.1029/2007JC004660.
Gan, J. P., L. Li, D. X. Wang, and X. G. Guo (2009b), Interaction of a river plume with coastal upwelling in the northeastern South China Sea, *Cont. Shelf Res.*, *29*(4), 728–740.
Gan, J. P., H. Ho, and L. L. Liang (2013), Dynamics of intensified downwelling circulation over a widened shelf in the northeastern South China Sea, *J. Phys. Oceanogr.*, *43*(1), 80–94.
Gan, J. P., J. J. Wang, L. L. Liang, L. Li, and X. G. Guo (2015), A modeling study of the formation, maintenance, and relaxation of upwelling circulation on the northeastern South China Sea shelf, *Deep Sea Res., Part II*, *117*(SI), 41–52.
Gopalakrishnan, G., B. D. Cornuelle, G. Gawarkiewicz, and J. L. McClean (2013), Structure and evolution of the cold dome off northeastern Taiwan: A numerical study, *Oceanography*, *26*(1), 66–79.
Gu, Y. Z., J. Y. Pan, and H. Lin (2012), Remote sensing observation and numerical modeling of an upwelling jet in Guangdong coastal water, *J. Geophys. Res.*, *117*, C08019, doi:10.1029/2012JC007922.
Gu, Y. Z., J. Y. Pan, and P. L. Li (2015), Remote sensing studies of an upwelling jet in Guangdong coastal water, *IEEE J. Sel. Top. Appl. Earth Obs. Remote Sens.*, *8*(1), 160–170.
Guo, J. J., W. D. Fang, G. H. Fang, and H. Y. Chen (2006), Variability of surface circulation in the South China Sea from satellite altimeter data, *Chin. Sci. Bull.*, *51*(2), 1–8.
He, Z. G., D. X. Wang, and J. Y. Hu (2002), Features of eddy kinetic energy and variations of upper circulation in the South China Sea, *Acta Oceanol. Sin.*, *21*(2), 305–314.
Hein, H., B. Hein, T. Pohlmann, and B. H. Long (2013), Inter-annual variability of upwelling off the South-Vietnamese coast and its relation to nutrient dynamics, *Global Planet. Change*, *110*(SI), 170–182.
Ho, C.-R., N.-J. Kuo, Q. Zheng, and Y. S. Soong (2000a), Dynamically active areas in the South China Sea detected from TOPEX/POSEIDON satellite altimeter data, *Remote Sens. Environ.*, *71*(3), 320–328.
Ho, C.-R., Q. A. Zheng, Y. S. Soong, N.-J. Kuo, and J.-H. Hu (2000b), Seasonal variability of sea surface height in the South China Sea observed with TOPEX/Poseidon altimeter data, *J. Geophys. Res.*, *105*, 13,981–13,990, doi:10.1029/2000JC900001.
Hong, H. S., C. Y. Zhang, S. L. Shang, B. Q. Huang, Y. H. Li, X. D. Li, and S. M. Zhang (2009), Interannual variability of summer coastal upwelling in the Taiwan Strait, *Cont. Shelf Res.*, *29*, 479–484.
Hong, H. S., C. T. A. Chen, Y. W. Jiang, J. Y. Lou, Z. Z. Chen, and J. Zhu (2011a), Source water of two-pronged northward flow in the southern Taiwan Strait in summer, *J. Oceanogr.*, *67*(4), 385–393.
Hong, H. S., F. Chai, C. Y. Zhang, B. Q. Huang, Y. W. Jiang, and J. Y. Hu (2011b), An overview of physical and biogeochemical processes and ecosystem dynamics in the Taiwan Strait, *Cont. Shelf Res.*, *31*, S3–S12.
Hu, J. Y., and H. Kawamura (2004), Detection of cyclonic eddy generated by looping tropical cyclone in the northern South China Sea: A case study, *Acta Oceanol. Sin.*, *23*(2), 213–224.
Hu, J. Y., H. Kawamura, H. S. Hong, and Y. Q. Qi (2000), A review on the currents in the South China Sea: Seasonal circulation, South China Sea Warm Current and Kuroshio intrusion, *J. Oceanogr.*, *56*(6), 607–624.
Hu, J. Y., H. Kawamura, H. S. Hong, M. Suetsugu, and M. Lin (2001), Hydrographic and satellite observations of summertime upwelling in the Taiwan Strait: A preliminary description, *Terr. Atmos. Oceanic Sci.*, *12*(2), 415–430.
Hu, J. Y., H. Kawamura, and D. L. Tang (2003a), Tidal front around the Hainan Island, northwest of the South China Sea, *J. Geophys. Res.* *108*(C11), 3342, doi:10.1029/2003JC001883.
Hu, J. Y., H. Kawamura, H. S. Hong, and W. R. Pan (2003b), A review of research on the upwelling in the Taiwan Strait, *Bull. Mar. Sci.*, *73*(3), 605–628.

Hu, J. Y., H. Kawamura, C. Y. Li, H. S. Hong, and Y. W. Jiang (2010), Review on current and seawater volume transport through the Taiwan Strait, *J. Oceanogr.*, *66*(5), 591–610.
Hu, J. Y., H. S. Hong, Y. Li, Y. W. Jiang, Z. Z. Chen, J. Zhu, Z. W. Wan, Z. Y. Sun, and H. X. Liang (2011a), Variable temperature, salinity and water mass structures in the southwestern Taiwan Strait in summer, *Cont. Shelf Res.*, *31*, S13–S23.
Hu, J. Y., J. P. Gan, Z. Y. Sun, J. Zhu, and M. H. Dai (2011b), Observed three-dimensional structure of a cold eddy in the southwestern South China Sea, *J. Geophys. Res.*, *116*, C05016, doi:10.1029/2010JC006810.
Hu, M. N., and C. F. Zhao (2007), Long-time observation of upwelling in the Zhoushan Islands and adjacent seas during the summer season [in Chinese with English abstract], *Period. Ocean Univ. China*, *37*(S1), 235–240.
Hu, M. N., and C. F. Zhao (2008), Upwelling in Zhejiang coastal areas during summer detected by satellite observations, *J. Remote Sens.*, *12*(2), 297–304.
Hwang, C. W., and S. A. Chen (2000), Circulations and eddies over the South China Sea derived from TOPEX/Poseidon altimetry, *J. Geophys. Res.*, *105*, 23,943–23,965, doi:10.1029/2000JC900092.
Isobe, A. (2008), Recent advances in ocean circulation research on the Yellow Sea and East China Sea shelves, *J. Oceanogr.*, *64*(4), 569–584.
Jan, S., C.-C. Chen, Y.-L. Tsai, Y. J. Yang, J. Wang, C.-S. Chern, G. Gawarkiewicz, R.-C. Lien, L. Centurioni, and J.-Y. Kuo (2011), Mean structure and variability of the cold dome northeast of Taiwan, *Oceanography*, *24*(SI), 100–109, doi:10.5670/oceanog.2011.98.
Jiang, X. P., Z. Zhong, and J. Jing (2009), Upper ocean response of the South China Sea to Typhoon Krovanh (2003), *Dyn. Atmos. Oceans*, *47*(1–3), 165–175.
Jiang, Y. W., F. Chai, Z. W. Wan, X. Zhang, and H. S. Hong (2011), Characteristics and mechanisms of the upwelling in the southern Taiwan Strait: A three-dimensional numerical model study, *J. Oceanogr.*, *67*, 699–708.
Jiao, N., Y. Zhang, K. Zhou, Q. Li, M. Dai, J. Liu, J. Guo, and B. Huang (2014), Revisiting the CO_2 "source" problem in upwelling areas—A comparative study on eddy upwellings in the South China Sea, *Biogeosciences*, *11*(9), 2465–2475.
Jing, Z. Y., Z. L. Hua, Y. Q. Qi, and X. H. Cheng (2007), Numerical study on the coastal upwelling and its seasonal variation in the East China Sea, *J. Coastal Res.*, *50*, 555–563.
Jing, Z. Y., Y. Q. Qi, Z. L. Hua, and H. Zhang (2009), Numerical study on the summer upwelling system in the northern continental shelf of the South China Sea, *Cont. Shelf Res.*, *29*(2), 467–478.
Jing, Z. Y., Y. Q. Qi, and Y. Du (2011), Upwelling in the continental shelf of northern South China Sea associated with 1997–1998 El Niño, *J. Geophys. Res.*, *116*, C02033, doi:10.1029/2010JC006598.
Jing, Z. Y., Y. Q. Qi, Y. Du, S. W. Zhang, and L. L. Xie (2015), Summer upwelling and thermal fronts in the northwestern South China Sea: Observational analysis of two mesoscale mapping surveys, *J. Geophys. Res. Oceans*, *120*, 1993–2006, doi:10.1002/2014JC010601.
Kuo, N.-J., and C.-R. Ho (2004), ENSO effect on the sea surface wind and sea surface temperature in the Taiwan Strait, *Geophys. Res. Lett.*, *31*, L13309, doi:10.1029/2004GL020303.
Kuo, N.-J., Q. A. Zheng, and C.-R. Ho (2000), Satellite observation of upwelling along the western coast of South China Sea, *Remote Sens. Environ.*, *74*, 463–470.
Kuo, N.-J., C.-R. Ho, and Q. A. Zheng (2004), Response of Vietnam coastal upwelling to the 1997–1998 ENSO event observed by multisensor data, *Remote Sens. Environ.*, *89*(1), 106–115.
Kuo, Y.-C., C.-S. Chern, J. Wang, and Y. L. Tsai (2011), Numerical study of upper ocean response to a typhoon moving zonally across the Luzon Strait, *Ocean Dyn.*, *61*(11), 1783–1795.
Lee, H.-J., and S.-Y. Chao (2003), A climatological description of circulation in and around the East China Sea, *Deep Sea Res., Part II*, *50*, 1065–1084.
Lentz, S. J. (2001), The influence of stratification on the wind-driven cross-shelf circulation over the north Carolina shelf, *J. Phys. Oceanogr.*, *31*(9), 2749–2760.
Lentz, S. J., and D. C. Chapman (2004), The importance of nonlinear cross-shelf momentum flux during wind-driven coastal upwelling, *J. Phys. Oceanogr.*, *34*(11), 2444–2457.
Li, L., J. Xu, C. Jing, R. Wu, and X. Guo (2003), Annual variation of sea surface height, dynamic topography and circulation in the South China Sea—A TOPEX/Poseidon satellite altimetry study, *Sci. China Ser. D*, *46*(2), 127–138.
Li, Y. H., X. H. Xu, X. J. Yin, J. Y. Fang, W. Y. Hu, and J. Chen (2015), Remote-sensing observations of Typhoon Soulik (2013) forced upwelling and sediment transport enhancement in the northern Taiwan Strait, *Int. J. Remote Sens.*, *36*(8), 2201–2218.
Li, Y. N., S. Q. Peng, W. Yang, and D. X. Wang (2012), Numerical simulation of the structure and variation of upwelling off the east coast of Hainan Island using QuikSCAT winds, *Chin. J. Oceanol. Limnol.*, *30*(6), 1068–1081.
Liang, X. S., and A. R. Robinson (2009), Multiscale processes and nonlinear dynamics of the circulation and upwelling events off Monterey Bay, *J. Phys. Oceanogr.*, *39*(2), 290–313.
Liao, G. H., Y. C. Yuan, and X. H. Xu (2008), Three dimensional diagnostic study of the circulation in the South China Sea during winter 1998, *J. Oceanogr.*, *64*(5), 803–814.
Lin, I.-I., W. T. Liu, C.-C. Wu, G. T. F. Wong, C. Hu, Z. Chen, W.-D. Liang, Y. Yang, and K.-K. Liu (2003a), New evidence for enhanced ocean primary production triggered by tropical cyclone, *Geophys. Res. Lett.*, *30*(13), 1718, doi:10.1029/2003GL017141.
Lin, I.-I., W. T. Liu, C.-C. Wu, J. C. H. Chiang, and C.-H. Sui (2003b), Satellite observations of modulation of surface winds by typhoon-induced upper ocean cooling, *Geophys. Res. Lett.*, *30*(3), 1131, doi:10.1029/2002GL015674.
Lin, P. G., J. Y. Hu, Q. A. Zheng, Z. Y. Sun, and J. Zhu (2016a), Observation of summertime upwelling off the eastern and northeastern coasts of Hainan Island, China, *Ocean Dyn.*, *66*(3), 387–399.
Lin, P. G., P. Cheng, J. P. Gan, and J. Y. Hu (2016b), Dynamics of wind-driven upwelling off the northeastern coast of Hainan Island, *J. Geophys. Res. Oceans*, *121*, 1160–1173, doi:10.1002/2015JC011000.
Liu, J. F., K. X. Mao, M. Yan, X. D. Zhang, and Y. J. Shi (2006), The general distribution characteristics of Luzon cold eddy [in Chinese with English abstract], *Mar. Forecasts*, *23*(2), 39–44.
Liu, Y., Z. C. Peng, G. J. Wei, T. G. Chen, W. D. Sun, J. F. He, R. Y. Sun, and G. J. Liu (2009), Variation of summer coastal upwelling at northern South China Sea during the last 100 years [in Chinese with English abstract], *Geochimica*, *38*(4), 317–322.
Liu, Y., Z. Peng, C.-C. Shen, R. Zhou, S. Song, Z. Shi, T. Chen, G. Wei, and K. L. DeLong (2013), Recent 121-year variability of western boundary upwelling in the northern South China Sea, *Geophys. Res. Lett.*, *40*, 3180–3183, doi:10.1002/grl.50381.
Liu, Z. Q., and J. P. Gan (2014), Modeling study of variable upwelling circulation in the East China Sea: Response to a coastal promontory, *J. Phys. Oceanogr.*, *44*(4), 1078–1094.
Liu, Z. Q., and J. P. Gan (2015), Upwelling induced by the frictional stress curl and vertical squeezing of the vortex tube over a submerged valley in the East China Sea, *J. Geophys. Res. Oceans*, *120*, 2571–2587, doi:10.1002/2015JC010715.

Lou, X. L., A. Q. Shi, Q. M. Xiao, and H. G. Zhang (2011), Satellite observation of the Zhejiang coastal upwelling in the East China Sea during 2007–2009, *Proc. SPIE*, *8175*(2), 283–304.
Lu, W. F., X.-H. Yan, and Y. W. Jiang (2015), Winter bloom and associated upwelling northwest of the Luzon Island: A coupled physical-biological modeling approach, *J. Geophys. Res. Oceans*, *120*, 533–546, doi:10.1002/2014JC010218.
Lü, X. G., F. L. Qiao, C. S. Xia, J. R. Zhu, and Y. L. Yuan (2006), Upwelling off Yangtze River estuary in summer, *J. Geophys. Res.*, *111*, C11S08, doi:10.1029/2005JC003250.
Lü, X. G., F. L. Qiao, C. S. Xia, and Y. L. Yuan (2007), Tidally induced upwelling off Yangtze River estuary and in Zhejiang coastal waters in summer, *Sci. China Ser. D: Earth Sci.*, *50*(3), 462–473.
Lü, X. G., F. L. Qiao, G. S. Wang, C. S. Xia, and Y. L. Yuan (2008), Upwelling off the west coast of Hainan Island in summer: Its detection and mechanisms, *Geophys. Res. Lett.*, *35*, L02604, doi:10.1029/2007GL032440.
Lü, X. G., F. L. Qiao, C. S. Xia, G. S. Wang, and Y. L. Yuan (2010), Upwelling and surface cold patches in the Yellow Sea in summer: Effects of tidal mixing on the vertical circulation, *Cont. Shelf Res.*, *30*(S), 620–632.
Macías, D., P. J. S. Franks, M. D. Ohman, and M. R. Landry (2012), Modeling the effects of coastal wind- and wind-stress curl-driven upwellings on plankton dynamics in the Southern California current system, *J. Mar. Syst.*, *94*, 107–119.
McGregor, H. V., M. Dima, H. W. Fischer, and S. Mulitza (2007), Rapid 20th-century increase in coastal upwelling off Northwest Africa, *Science*, *315*, 637–639.
Mei, W., C. C. Lien, I. I. Lin, and S.-P. Xie (2015), Tropical cyclone-induced ocean response: A comparative study of the South China Sea and Tropical Northwest Pacific, *J. Clim.*, *28*(15), 5952–5968.
Miao, X., and J. Y. Hu (2011), Analysis on characteristics of wind-driven coastal upwelling off the southeastern China coast using coastal upwelling index [in Chinese with English abstract], *Mar. Sci. Bull.*, *30*(3), 258–265.
Morimoto, A., S. Kojima, S. Jan, and D. Takahashi (2009), Movement of the Kuroshio axis to the northeast shelf of Taiwan during typhoon events, *Estuarine Coastal Shelf Sci.*, *82*(3), 547–552.
Pan, A. J., L. Li, X. G. Guo, and J. D. Xu (2012a), A preliminary study of the internal tide in the summertime upwelling regime off the Guangdong shelf edge in 2002 and its local feedback [in Chinese with English abstract], *J. Oceanogr. Taiwan Strait*, *31*(2), 151–159.
Pan, A. J., X. G. Guo, J. D. Xu, J. Huang, and X. F. Wan (2012b), Responses of Guangdong coastal upwelling to the summertime typhoons of 2006, *Sci. China Ser. D: Earth Sci.*, *55*(3), 495–506.
Pan, J. Y., and Y. J. Sun (2013), Estimate of ocean mixed layer deepening after a typhoon passage over the South China Sea by using satellite data, *J. Phys. Oceanogr.*, *43*(3), 498–506.
Pan, Y. P., and W. Y. Sha (2004), Numerical study on winter coastal upwelling off Fujian and Zhejiang coast [in Chinese with English abstract], *Oceanol. Limnol. Sin.*, *35*(3), 193–201.
Pei, S. F., Z. L. Shen, and E. A. Laws (2009), Nutrient dynamics in the upwelling area of Changjiang (Yangtze River) Estuary, *J. Coastal Res.*, *25*(3), 569–580.
Petrichenko, S. A. (2010), Using the databases of the ocean climate laboratory of the NODC NOAA for constructing climatology maps by the example of the upwelling area at the coast of Southern Vietnam, *Russ. Meteorol. Hydrol.*, *35*(7), 464–467.
Qiao, F. L. (2012), *Regional Oceanography of the China Seas: Physical Oceanography* [in Chinese], 300 pp., Ocean Press, Beijing.
Qiao, F. L., and X. G. Lü (2008), Coastal upwelling in the South China Sea, in *Satellite Remote Sensing of South China Sea*, edited by A. K. Liu, C. R. Ho, and C. T. Liu, pp. 135–158, Tingmao Publish Co, Taiwan.
Qiao, F. L., Y. Z. Yang, X. G. Lü, C. S. Xia, X. Y. Chen, B. D. Wang, and Y. L. Yuan (2006), Coastal upwelling in the East China Sea in winter, *J. Geophys. Res.*, *111*, C11S06, doi:10.1029/2005JC003264.
Qiao, F. L., W. Zhao, and X. G. Lü (2008), A ring-like structure of cold eddy in the East China Sea [in Chinese with English abstract], *Prog. Nat. Sci.*, *18*(6), 674–679.
Qu, T. (2000), Upper-layer circulation in the South China Sea, *J. Phys. Oceanogr.*, *30*, 1450–1460.
Shang, S. L., C. Y. Zhang, H. S. Hong, S. P. Shang, and F. Chai (2004), Short-term variability of chlorophyll associated with upwelling events in the Taiwan Strait during the southwest monsoon of 1998, *Deep Sea Res., Part II*, *51*(10–11), 1113–1127.
Shang, S. L., L. Li, F. Sun, J. Wu, C. Hu, D. Chen, X. Ning, Y. Qiu, C. Zhang, and S. P. Shang (2008), Changes of temperature and bio-optical properties in the South China Sea in response to Typhoon Lingling, 2001, *Geophys. Res. Lett.*, *35*, L10602, doi:10.1029/2008GL033502.
Shen, M.-L., Y.-H. Tseng, and S. Jan (2011), The formation and dynamics of the cold-dome off northeastern Taiwan, *J. Mar. Syst.*, *86*(1–2), 10–27.
Shih, Y.-Y., J.-S. Hsieh, G.-C. Gong, C.-C. Hung, W.-C. Chou, M.-A. Lee, K.-S. Chen, M.-H. Chen, and C.-R. Wu (2013), Field observations of changes in SST, Chlorophyll and POC flux in the Southern East China Sea before and after the passage of Typhoon Jangmi, *Terr. Atmos. Oceanic Sci.*, *24*(5), 899–910.
Shu, Y. Q., D. X. Wang, J. Zhu, and S. Q. Peng (2011), The 4-D structure of upwelling and Pearl River plume in the northern South China Sea during summer 2008 revealed by a data assimilation model, *Ocean Modell.*, *36*(3–4), 228–241.
Spall, M. A. (2008), Buoyancy-forced downwelling in boundary currents, *J. Phys. Oceanogr.*, *38*(12), 2704–2721.
Su, J., and T. Pohlmann (2009), Wind and topography influence on an upwelling system at the eastern Hainan coast, *J. Geophys. Res.*, *114*, C06017, doi:10.1029/2008JC005018.
Su, J., J. Wang, T. Pohlmann, and D. F. Xu (2011), The influence of meteorological variation on the upwelling system off eastern Hainan during summer 2007–2008, *Ocean Dyn.*, *61*(6), 717–730.
Su, J., M. Q. Xu, T. Pohlmann, D. F. Xu, and D. R. Wang (2013), A western boundary upwelling system response to recent climate variation (1960–2006), *Cont. Shelf Res.*, *57*(SI), 3–9.
Sun, C. X., and Q. Y. Liu (2011), Double eddy structure of the winter Luzon cold eddy based on satellite altimeter data [in Chinese with English abstract], *J. Trop. Oceanogr.*, *30*(3), 9–15.
Tang, D. L., D. R. Kester, I. H. Ni, H. Kawamura, and H. S. Hong (2002), Upwelling in the Taiwan Strait during the summer monsoon detected by satellite and shipboard measurements, *Remote Sens. Environ.*, *83*(3), 457–471.
Tang, D. L., H. Kawamura, and L. Guan (2004a), Long-time observation of annual variation of Taiwan Strait upwelling in summer season, *Adv. Space Res.*, *33*(3), 307–312.
Tang, D. L., H. Kawamura, T. V. Dien, and M. A. Lee (2004b), Offshore phytoplankton biomass increase and its oceanographic causes in the South China Sea, *Mar. Ecol. Prog. Ser.*, *268*, 31–41.
Tsai, Y. L., C.-S. Chern, and J. Wang (2008), Typhoon induced upper ocean cooling off northeastern Taiwan, *Geophys. Res. Lett.*, *35*, L14605, doi:10.1029/2008GL034368.
Tseng, Y. F., J. Lin, M. Dai, and S. J. Kao (2014), Joint effect of freshwater plume and coastal upwelling on phytoplankton growth off the Changjiang River, *Biogeosciences*, *11*(2), 409–423.

Tseng, Y. H., S. Jan, D. E. Dietrich, I.-I. Lin, Y.-T. Chang, and T.-Y. Tang (2010), Modeled oceanic response and sea surface cooling to Typhoon Kai-Tak, *Terr. Atmos. Oceanic Sci.*, *21*(1), 85–98.

Tseng, Y.-H., M.-L. Shen, S. Jan, D. E. Dietrich, and C.-P. Chiang (2012), Validation of the Kuroshio Current System in the dual-domain Pacific Ocean, *Prog. Oceanogr.*, *105*, 102–124.

Udarbe-Walker, M. J. B., and C. L. Villanoy (2001), Structure of potential upwelling areas in the Philippines, *Deep Sea Res., Part I*, *48*, 1499–1518.

Wan, X. F., A. J. Pan, X. G. Guo, C. S. Jing, and J. Huang (2013), Seasonal variation features of the hydrodynamic environment in the western Taiwan Strait [in Chinese with English abstract], *J. Appl. Oceanogr.*, *32*(2), 156–163.

Wang, D. K., H. Wang, M. Li, G. M. Liu, and X. Y. Wu (2013), Role of Ekman transport versus Ekman pumping in driving summer upwelling in the South China Sea, *J. Ocean Univ. China*, *12*(3), 355–365.

Wang, D. X., B. Hong, J. P. Gan, and H. Z. Xu (2010), Numerical investigation on propulsion of the counter-wind current in the northern South China Sea in winter, *Deep Sea Res., Part I*, *57*(10), 1206–1221.

Wang, D. X., W. Zhuang, S.-P. Xie, J. Hu, Y. Shu, and R. Wu (2012), Coastal upwelling in summer 2000 in the northeastern South China Sea, *J. Geophys. Res.*, *117*, C04009, doi:10.1029/2011JC007465.

Wang, D. X., Y. Q. Shu, H. J. Xue, J. Y. Hu, J. Chen, and W. Zhuang (2014), Relative contributions of local wind and topography to the coastal upwelling in the northern South China Sea, *J. Geophys. Res. Oceans*, *119*, 2550–2567, doi:10.1002/2013JC009172.

Wang, G. H., J. L. Su, and P. Chu (2003), Mesoscale eddies in the South China Sea observed with altimeter data, *Geophys. Res. Lett.* *30*(21), 2121, doi:10.1029/2003GL018532.

Wang, G. S., and F. L. Qiao (2008), Ocean temperature responses to Typhoon Mstsa in the East China Sea, *Acta Oceanol. Sin.*, *27*, 26–38.

Wang, H., G. M. Liu, S. Sun, B. P. Han, and X. Fu (2007), A three-dimensional coupled physical and biological model study in the spring of 1993 in Bohai Sea of China, *Acta Oceanol. Sin.*, *26*(6), 1–12.

Wang, J., H. Hong, Y. Jiang, F. Chai, and X.-H. Yan (2013), Summer nitrogenous nutrient transport and its fate in the Taiwan Strait: A coupled physical-biological modeling approach, *J. Geophys. Res. Oceans*, *118*, 4184–4200, doi:10.1002/jgrc.20300.

Wang, J. J., D. L. Tang, and Y. Sui (2010), Winter phytoplankton bloom induced by subsurface upwelling and mixed layer entrainment southwest of Luzon Strait, *J. Mar. Syst.*, *83*(SI), 141–149.

Wang, T. T., J. C. Kang, W. J. Li, H. R. Ren, D. An, and F. Meng (2008), Three-dimension temperature structure of cold eddy-upwelling system off northeastern Taiwan Island in summer and winter [in Chinese with English abstract], *J. Trop. Oceanogr.*, *27*(6), 6–13.

Wei, G. F., D. L. Tang, and S. F. Wang (2008), Distribution of chlorophyll and harmful algal blooms (HABs): A review on space based studies in the coastal environments of Chinese marginal seas, *Adv. Space Res.*, *41*, 12–19.

Wei, Q. S., J. Y. Zang, R. Zhan, and R. X. Li (2011), Characteristics of the ecological environment in upwelling area northeast of the Changjiang River Estuary [in Chinese with English abstract], *Oceanol. Limnol. Sin.*, *42*(6), 899–905.

Wei, Z. X., C. Y. Li, G. H. Fang, and X. Y. Wang (2003), Numerical diagnostic study of the summertime circulation in the Bohai Sea and the water transport in the Bohai Strait [in Chinese with English abstract], *Adv. Mar. Sci.*, *21*(4), 454–464.

Wong, G. T. F., S.-Y. Chao, Y.-H. Li, and F.-K. Shiah (2000), The Kuroshio edge exchange processes (KEEP) study—An introduction to hypotheses and highlights, *Cont. Shelf Res.*, *20*, 335–347.

Wong, G. T. F., C.-C. Hung, and G.-C. Gong (2004), Dissolved iodine species in the East China Sea—A complementary tracer for upwelling water on the shelf, *Cont. Shelf Res.*, *24*(13–14), 1465–1484.

Wu, C.-R., and C.-W. J. Chang (2005), Interannual variability of the South China Sea in a data assimilation model, *Geophys. Res. Lett.*, *32*, L17611, doi:10.1029/2005GL023798.

Wu, C.-R., H.-F. Lu, and S.-Y. Chao (2008), A numerical study on the formation of upwelling off northeast Taiwan, *J. Geophys. Res.*, *113*, C08025, doi:10.1029/2007JC004697.

Wu, R. S., and L. Li (2003), Summarization of study on upwelling system in the South China Sea [in Chinese with English abstract], *J. Oceanogr. Taiwan Strait*, *22*(2), 269–276.

Xiao, H., X. G. Guo, and R. S. Wu (2002), Summarization of studies on hydrographic characteristics in Taiwan Strait [in Chinese with English abstract], *J. Oceanogr. Taiwan Strait*, *21*(1), 126–138.

Xie, L. L., S. W. Zhang, and H. Zhao (2012), Overview of studies on Qiongdong upwelling [in Chinese with English abstract], *J. Trop. Oceanogr.*, *31*(4), 35–41.

Xie, S.-P., Q. Xie, D. Wang, and W. T. Liu (2003), Summer upwelling in the South China Sea and its role in regional climate variations, *J. Geophys. Res.*, *108*(C8), 3261, doi:10.1029/2003JC001867.

Xie, S.-P., C. H. Chang, Q. Xie, and D. X. Wang (2007), Intraseasonal variability in the summer South China Sea: Wind jet, cold filament, and recirculations, *J. Geophys. Res.*, *112*, C10008, doi:10.1029/2007JC004238.

Xiong, X. J., et al. (2012), *China Coastal Ocean: Physical Oceanography and Marine Meteorology* [in Chinese], 280 pp., Ocean Press, Beijing.

Xiu, S. M., and H. S. Huang (2006), Study on numerical simulation for upwelling of winter off northeastern Taiwan [in Chinese with English abstract], *J. Hydrodyn.*, *21*(3), 331–338.

Xiu, S. M., K. Wang, and P. G. Sun (2001), Study on the information of remote sensing for cold eddies and its variations in the sea area northeast of Taiwan—I. The seasonal variations of the cold eddies [in Chinese with English abstract], *J. Oceanogr. Huanghai Bohai Seas*, *19*(2), 57–64.

Xiu, S. M., Q. A. Zheng, and X. P. Sun (2002), Shelf upwelling induced by mesoscale eddy, *J. Hydrodyn.*, *17*(1), 61–68.

Xu, J. D., S. Z. Cai, L. L. Xiong, Y. Qiu, and D. Y. Zhu (2013), Study on coastal upwelling in eastern Hainan Island and western Guangdong in summer, 2006 [in Chinese with English abstract], *Acta Oceanol. Sin.*, *35*(4), 11–18.

Xu, J. D., S. Z. Cai, L. L. Xiong, Y. Qiu, X. W. Zhou, and D. Y. Zhu (2014), Observational study on summertime upwelling in coastal seas between eastern Guangdong and southern Fujian [in Chinese with English abstract], *J. Trop. Oceanogr.*, *33*(2), 1–9.

Yan, Y. W., Z. Ling, and C. L. Chen (2015), Winter coastal upwelling off northwest Borneo in the South China Sea, *Acta Oceanol. Sin.*, *34*(1), 3–10.

Yang, D. Z., B. Yin, Z. Liu, and X. Feng (2011), Numerical study of the ocean circulation on the East China Sea shelf and a Kuroshio bottom branch northeast of Taiwan in summer, *J. Geophys. Res.*, *116*, C05015, doi:10.1029/2010JC006777.

Yang, D. Z., B. Yin, J. Sun, and Y. Zhang (2013), Numerical study on the origins and the forcing mechanism of the phosphate in upwelling areas off the coast of Zhejiang Province, China in summer, *J. Mar. Syst.*, *123*, 1–18.

Yang, Y. J., L. Sun, A. M. Duan, Y. B. Li, Y. F. Fu, Y. F. Yan, Z. Q. Wang, and T. Xian (2012), Impacts of the binary typhoons on upper ocean environments in November 2007, *J. Appl. Remote Sens. 6*, 063583.

Yang, Y. L., S.-P. Xie, Y. Du, and H. Tokinaga (2015), Interdecadal difference of interannual variability characteristics of South China Sea SSTs associated with ENSO, *J. Clim.*, *28*(18), 7145–7160.

Ye, H. J., Y. Sui, D. L. Tang, and Y. D. Afanasyev (2013), A subsurface chlorophyll *a* bloom induced by typhoon in the South China Sea, *J. Mar. Syst.*, *128*, 138–145.

Yuan, Y. C., X. W. Bu, G. H. Liao, R. Y. Lou, J. L. Su, and K. S. Wang (2004), Diagnostic calculation of the upper-layer circulation in the South China Sea during the winter of 1998, *Acta Oceanogr. Sin.*, *23*(2), 187–199.

Zhang, C. Y., H. S. Hong, C. M. Hu, and S. L. Shang (2011), Evolution of a coastal upwelling event during summer 2004 in the southern Taiwan Strait, *Acta Oceanol. Sin.*, *30*(1), 1–6.

Zhang, S. W., C. S. Xia, and Y. L. Yuan (2002), Effect of the upwelling current on the vertical chlorophyll distribution in the Yellow Sea cold water mass [in Chinese with English abstract], *Adv. Mar. Sci.*, *20*(3), 9–14.

Zhao, B. R., G. F. Ren, D. M. Cao, and Y. L. Yang (2001), Characteristics of the ecological environment in upwelling area adjacent to the Changjiang River estuary [in Chinese with English abstract], *Oceanol. Limnol. Sin.*, *32*(3), 327–333.

Zhao, H., D. D. Sui, Q. Xie, G. Q. Han, D. X. Wang, N. Chen, and D. L. Tang (2012), Distribution and interannual variation of winter phytoplankton blooms northwest of Luzon Islands from satellite observations, *Aquat. Ecosyst. Health Manage.*, *15*(1), 53–61.

Zhao, H., G. Q. Han, S. W. Zhang, and D. X. Wang (2013), Two phytoplankton blooms near Luzon Strait generated by lingering Typhoon Parma, *J. Geophys. Res. Biogeosci.*, *118*, 412–421, doi:10.1002/jgrg.20041.

Zheng, C. W. (2011), Sea surface wind field analysis in the China seas during the last 22 years with CCMP wind field [in Chinese with English abstract], *Meteorol. Disaster Reduct. Res.*, *34*(3), 41–46.

Zheng, G. M., and D. L. Tang (2007), Offshore and nearshore chlorophyll increases induced by typhoon winds and subsequent terrestrial rainwater runoff, *Mar. Ecol. Prog. Ser.*, *333*, 61–74.

Zheng, Q. A., G. Fang, and Y. T. Song (2006), Introduction to special section: Dynamics and circulation of the Yellow, East, and South China Seas, *J. Geophys. Res.*, *111*, C11S01, doi:10.1029/2005JC003261.

Zhu, J., J. Y. Hu, and Z. Y. Liu (2013), On summer stratification and tidal mixing in the Taiwan Strait, *Front. Earth Sci.*, *7*(2), 141–150.

Zhu, J. R. (2003), Dynamic mechanism of the upwelling on the west side of the submerged river valley off the Changjiang mouth in summertime, *Chin. Sci. Bull.*, *48*(24), 2754–2758.

Zhu, J. R., P. X. Ding, and D. X. Hu (2003), Observation of the diluted water and plume front off the Changjiang River estuary during August 2000 [in Chinese with English abstract], *Oceanol. Limnol. Sin.*, *34*(3), 249–255.

Zhu, Z. F., and J. S. Yu (2014), Estimating the occurrence of wind-driven coastal upwelling associated with "Aoshio" on the northeast shore of Tokyo Bay, Japan: An analytical model, *Sci. World J.*, *2014*, 769823.

Zhuang, W., D. X. Wang, J. Y. Hu, and W. S. Ni (2006), Response of the cold water mass in the western South China Sea to the wind stress curl associated with the summer monsoon, *Acta Oceanol. Sin.*, *25*(4), 1–13.